Attosecond electronic and nuclear quantum photodinamics in neutral triatomic system

Gábor J. Halász[(1)] and Ágnes Vibók[(2)]

[(1)]Institute of Informatics, University of Debrecen,
H-4010 Debrecen, PO Box 5, HUNGARY

[(2)]Department of Theoretical Physics, University of Debrecen,
H-4010 Debrecen, PO Box 5, HUNGARY
vibok@phys.unideb.hu

Numerical Simulation of an attosecond UV-XUV

Pump-probe experiment on the neutral ozone

molecule

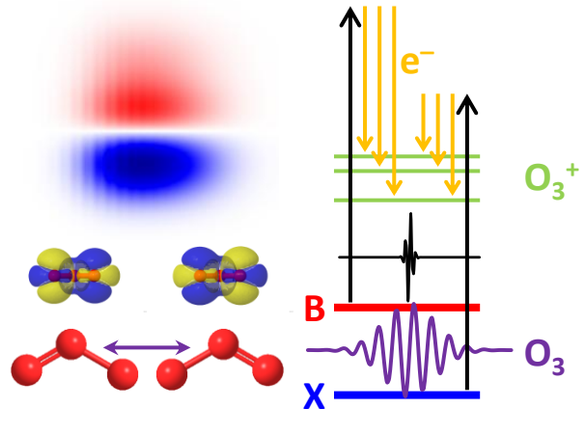

- Electron dynamics in molecules in most of the time are strongly coupled to nuclear dynamics. Proper theoretical description of them in polyatomic molecules is a challenge.

- We propose a new scheme for the description of the coupled electron and nuclear motion in the ozone molecule.

- The electron dynamics as well as the nuclear dynamics will be treated separately.

The electronic structure of the molecule

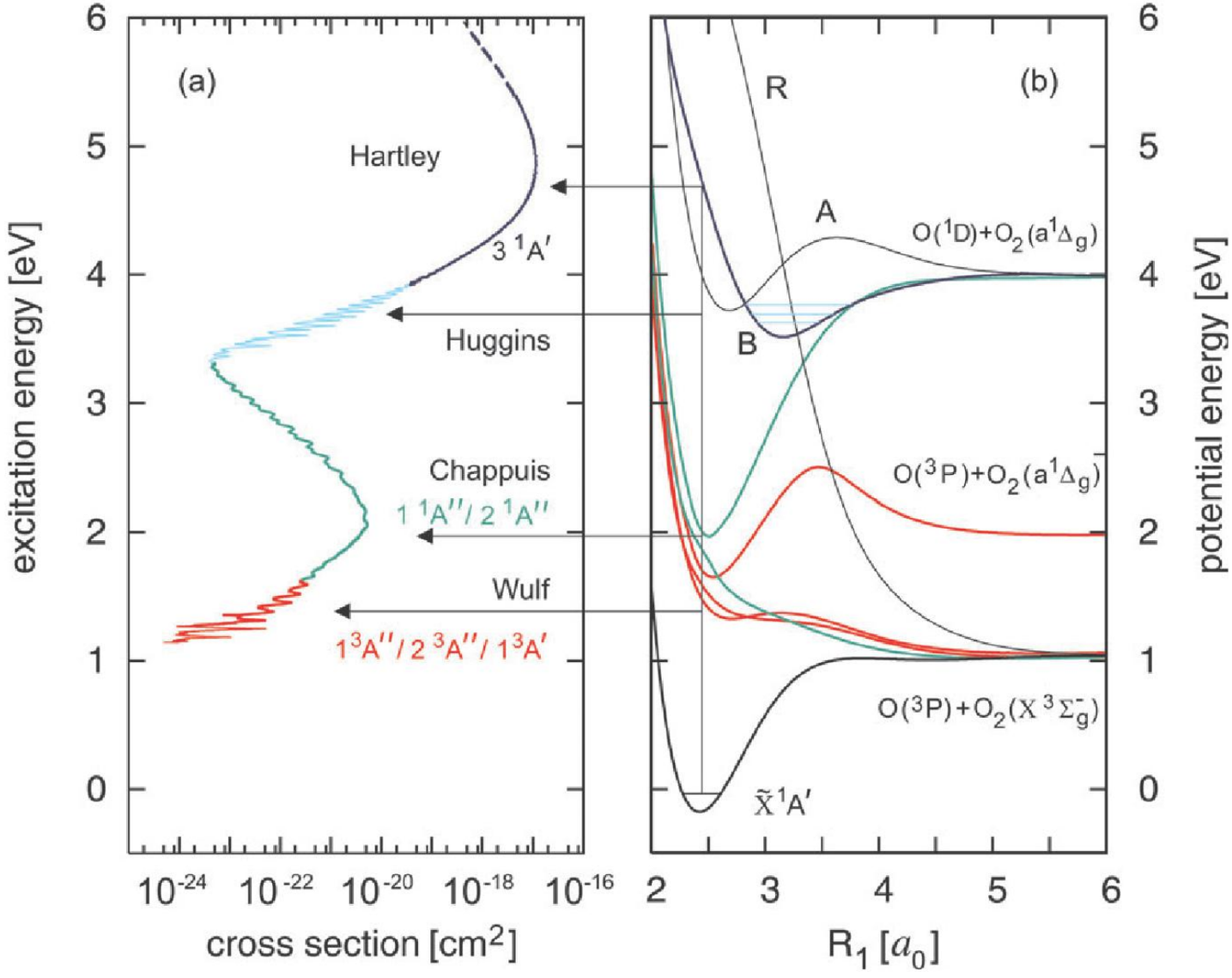

Preparing initial coherent non stationary state by pump pulses;

*.

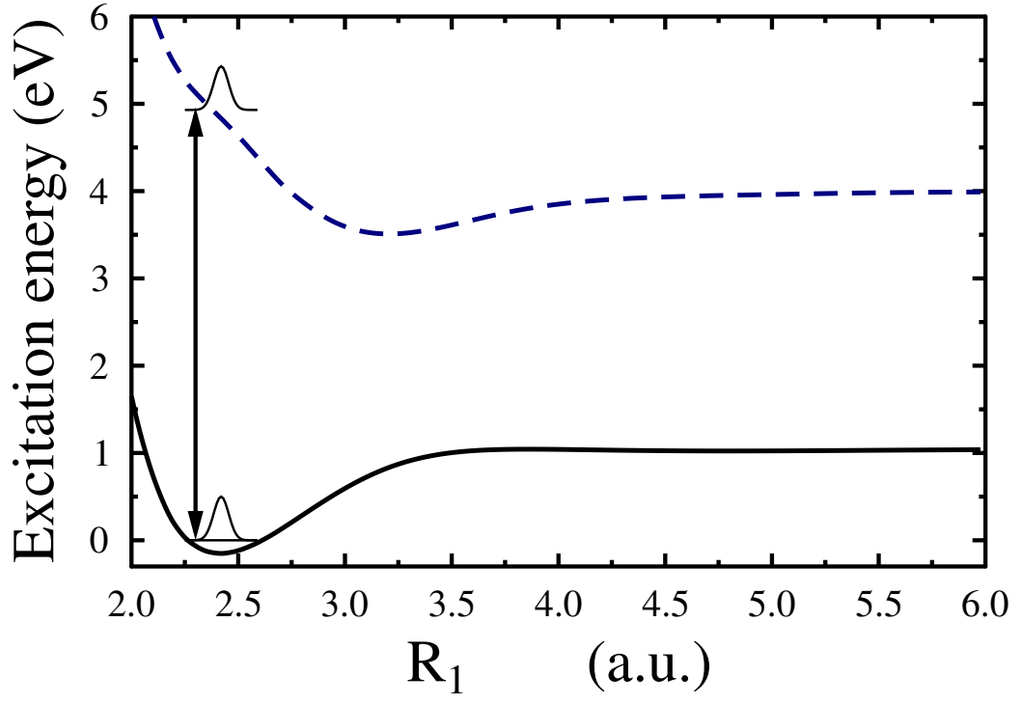

It is a superposition of ground and the Hartley † states (which is populated by means of few-cycle 3rd harmonic pulses of Ti:Sa-lasers.)

Neither the electrons nor the nuclei are in a stationary state.

(The center wavelength $\lambda = 260$ nm, FWHM is 3 fs and I= $10^{13} W/cm^2$.)

*G. J. Halász, A. Perveaux, B. Lasorne, M. A. Robb, F. Gatti and Á. V., PRA **88**, 023425 (2013).

†S. Y. Grebenshchikov, Z-W. Qu, H. Zhu and R. Schinke, Phys. Chem. Chem Phys. **9**, 2044 (2007).

Time-dependent Born–Oppenheimer Separation

The total wave function of the molecular system Ψ_{tot} can be assumed as:

$$\Psi_{tot}(\vec{r}_{el}, \vec{R}, t) = \sum_{k=1}^{n} \Psi_{nuc}^{k}(\vec{R}, t)\psi_{el}^{k}(\vec{r}_{el}; \vec{R})$$

- $\Psi_{nuc}^{k}(\vec{R}, t)$ is the nuclear wave function;
- $\psi_{el}^{k}(\vec{r}; \vec{R})$ is the electronic wave function;
- n is the number of the molecular electronic states (now $n = 4$);

Nuclear Dynamics

$$i\frac{\partial}{\partial t}\Psi^k_{nuc}(\vec{R},t) = \sum_l H_{k,l}\Psi^l_{nuc}(\vec{R},t)$$

where

$$H = T_{nuc} + V + K$$

- T_{nuc} is the nuclear kinetic energy;
- $V_{k,k}$ $(k = 1, ...n)$ is the $k-th$ B-O potential;
- $K_{k,l}$ with $k \neq l$ is the light-matter coupling $(\vec{\mu}(k,l) \cdot \vec{E}(t))$;

The nuclear Schrödinger equation is solved by using the MCTDH (multi configuration time dependent Hartree) method*.

It is very efficient approach for solving the TD nuclear Schrödinger equation. Molecules with 25-30 modes can be described by using it.

We have n electronic diabatic states ($k = 1$, ground and $k = 2, ..., n$ excited). The MCTDH nuclear wave function for the $k-th$ state is $\Psi^k_{nuc}(\vec{R}, t)$ and contains the relative phases between the electronic states:

$$\Psi^k_{nuc}(\vec{R}, t) = \exp(-i\phi_k(\vec{R}, t))a_k(\vec{R}, t)$$

$\exp(-i\phi_k(\vec{R}, t))$ is the phase of the $k-th$ state, which oscillates very fast. $\Psi^k_{nuc}(\vec{R}, t)$ coefficients are provided by the MCTDH and contain all the information about the phases.

*H.-D. Meyer, U. Manthe, and L. S. Cederbaum, *Chem. Phys. Lett.* **165**, 73 (1990); U. Manthe, H.-D. Meyer, and L. S. Cederbaum, J. Chem. Phys. **97**, 3199 (1992); M. H. Beck, A. Jäckle, G. A. Worth, and H.-D. Meyer, Phys. Rep. **324**, 1 (2000); Worth, G. A.; et al., The MCTDH Package, Version 8.2, (2000), Version 8.3, (2002), Version 8.4 (2007), University of Heidelberg, Germany; See http://mctdh.uni-hd.de/; H.-D. Meyer, F. Gatti, and G. A. Worth, Eds.; Multidimensional Quantum Dynamics: MCTDH Theory and Applications. Wiley-VCH, Weinheim, (2009).

The TD density operator is*:

$$\widehat{\rho}(\vec{R},\vec{R}',t) = \left|\Psi_{tot}(\vec{r},\vec{R}\,,t)\right\rangle\left\langle\Psi_{tot}(\vec{r},\vec{R}',t)\right|,$$

the density matrix can be defined as:

$$\rho_{ii}(\vec{R},\vec{R}',t) = \left\langle\psi^i_{el}(\vec{r};\vec{R}\,)\right|\widehat{\rho}(\vec{R},\vec{R}',t)\left|\psi^i_{el}(\vec{r};\vec{R}')\right\rangle = \Psi^i_{nuc}(\vec{R},t)\Psi^{i*}_{nuc}(\vec{R}',t).$$

The population on the $i-th$ state is:

$$P_{ii}(t) = \int d\vec{R}\rho_{ii}(\vec{R},\vec{R},t).$$

*G. J. Halász, A. Perveaux, B. Lasorne, M. A. Robb, F. Gatti and Á. V., *PRA* **86**, 043426 (2012); G. J. Halász, A. Perveaux, B. Lasorne, M. A. Robb, F. Gatti and Á. V., *PRA* **88**, 023425 (2013).

The density matrix element over the $i-th$ and $i^{'}-th$ molecular electronic states is:

$$\rho_{ii'}(\vec{R},\vec{R}',t) = \left\langle \psi^{i}_{el}(\vec{r};\vec{R}) \right| \widehat{\rho}(\vec{R},\vec{R}',t) \left| \psi^{i^{'}}_{el}(\vec{r};\vec{R}') \right\rangle = \Psi^{i}_{nuc}(\vec{R},t)\Psi^{i'*}_{nuc}(\vec{R}',t),$$

The relative electronic coherence between the $i-th$ and $i^{'}-th$ states is *:

$$C_{ii'}(t) = \int d\vec{R}\rho_{ii'}(\vec{R},\vec{R},t)/\sqrt{P_i(t)P_{i'}(t)}.$$

*G. J. Halász, A. Perveaux, B. Lasorne, M. A. Robb, F. Gatti and Á. V., *PRA* **86**, 043426 (2012); G. J. Halász, A. Perveaux, B. Lasorne, M. A. Robb, F. Gatti and Á. V., *PRA* **88**, 023425 (2013).

The applied electric field and the time evolution of the diabatic populations on the ground (X) and diabatic excited (B) states*

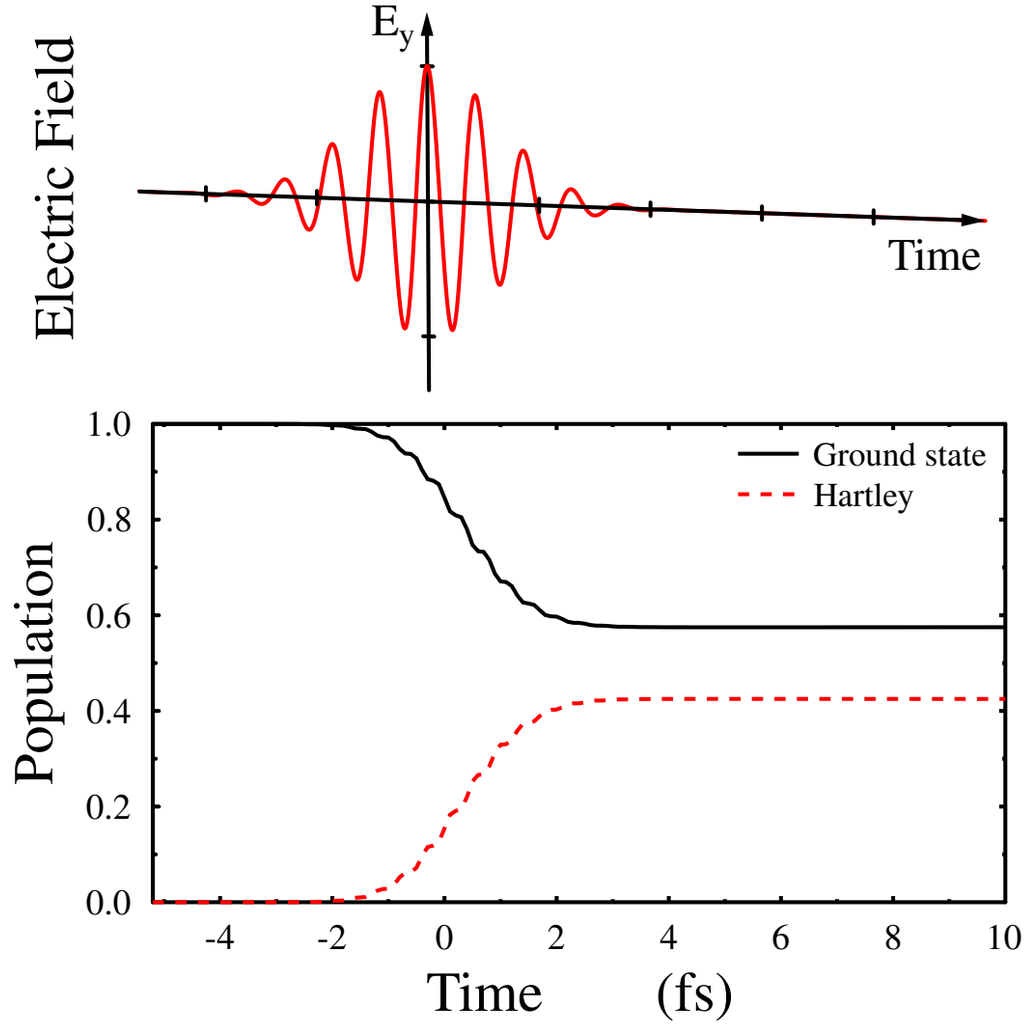

*G. J. Halász, A. Perveaux, B. Lasorne, M. A. Robb, F. Gatti and Á. V., PRA **88**, 023425 (2013).

The real, the imaginary parts and the absolute value of the relative electronic coherence between the ground (X) and Hartley (B) states

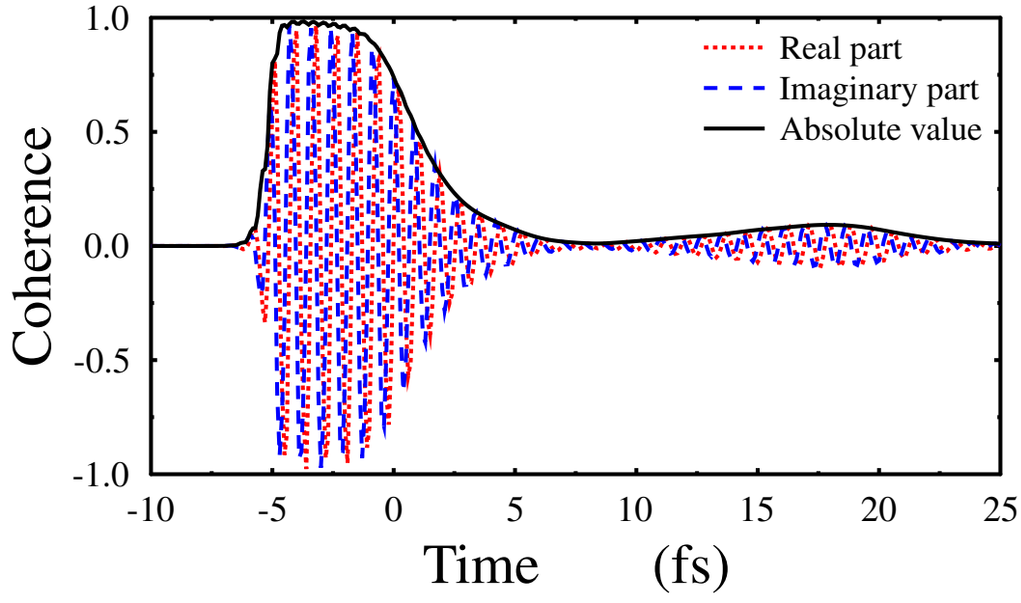

- In the first time period the coherence increases very fast and reaches its maximum;
- It retains this value for 3 - 4 fs, which is approximately equivalent to the duration of the laser pulse;
- A few femtoseconds later ($\sim$ 5 fs), the coherence reappears in contrast with what was observed in previously;
- This phenomenon could be enhanced experimentally by optimizing the parameters of the laser pulse;

The two-dimensional nuclear density function (depending on R_1 and R_2, the two bond lengths, and integrated over θ, the bond angle) is:

$$\left|\Psi^i_{nuc}(R_1, R_2, t)\right|^2 = \int \Psi^i_{nuc}(R_1, R_2, \theta, t)\Psi^{i*}_{nuc}(R_1, R_2, \theta, t)\sin\theta d\theta$$

Snapshots of the time evolution of the nuclear wave packet density along both

O - O bonds*

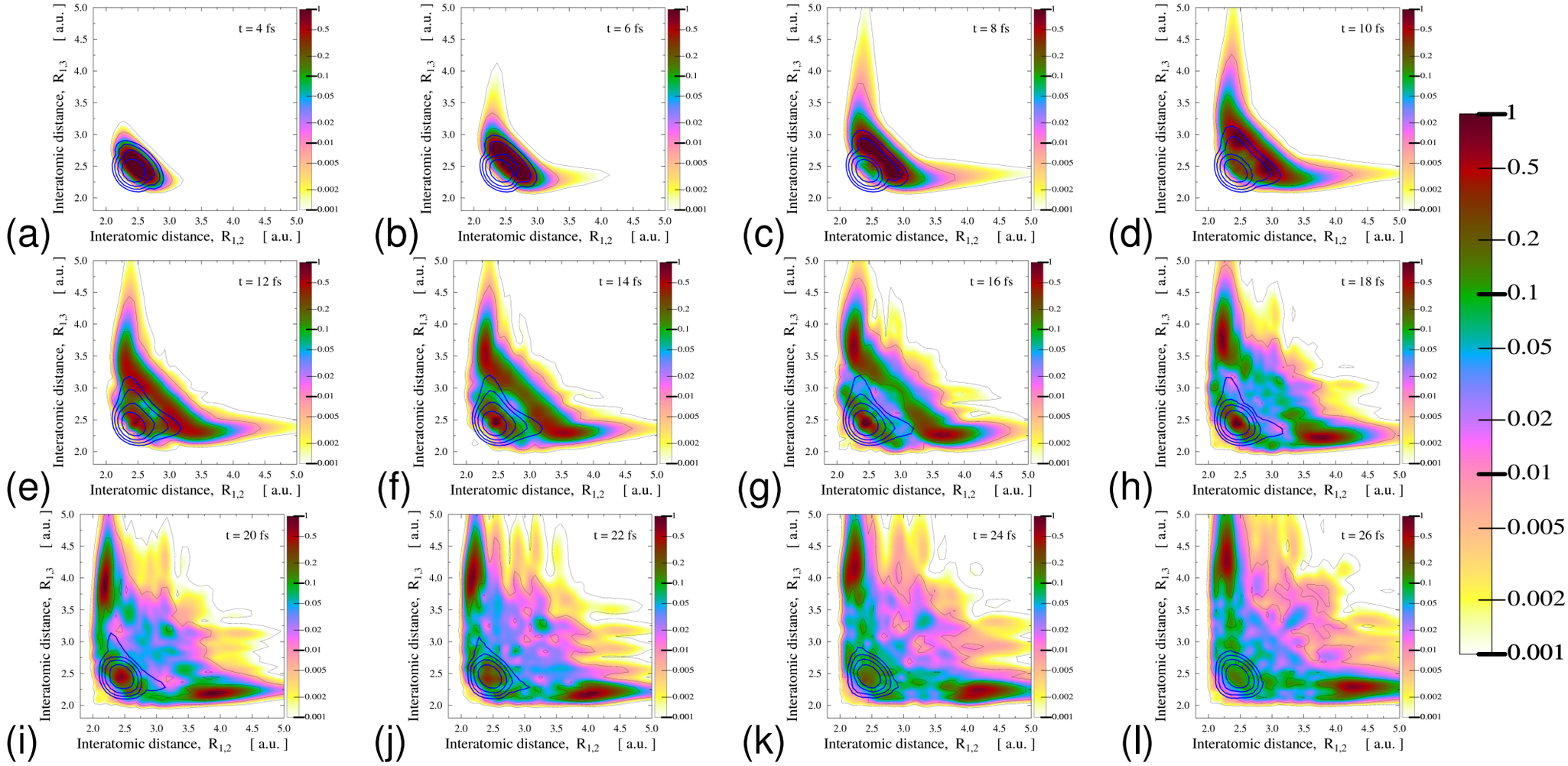

*G. J. Halász, A. Perveaux, B. Lasorne, M. A. Robb, F. Gatti and Á. V., PRA **88**, 023425 (2013).

Electronic structure part

Details of the QC calculations

- Gaussian and Molpro packages were used;
- SA-4-CASSCF(18,12)/STO-3G;
- Various schemes of state-averaging were used depending on the number of coupled states;
- Here we state-averaged over X and B;
- Larger basis set were also tried (aug-cc-pVTZ and perhaps even larger). Results do not change when looking at the electronic wavepacket;
- MRCI calculations were also performed to check that the CASSCF calculations where correct in terms of electronic wavefunctions;

The excited state differential electronic charge density at the FC geometry (difference of the total charge density between the excited state B and the ground state):

$$
\begin{aligned}
& \Delta\rho^B(\vec{r},t;\vec{R}_{FC}) = \rho^{tot}(\vec{r},t;\vec{R}_{FC}) - [|\Psi^X_{nuc}(\vec{R}_{FC},t)|^2 + |\Psi^B_{nuc}(\vec{R}_{FC},t)|^2]\rho^X(\vec{r};\vec{R}_{FC}) \\
= \;& |\Psi^B_{nuc}(\vec{R}_{FC},t)|^2[\rho^B(\vec{r};\vec{R}_{FC}) - \rho^X(\vec{r};\vec{R}_{FC})] + 2Re\Psi^{X*}_{nuc}(\vec{R}_{FC},t)\Psi^B_{nuc}(\vec{R}_{FC},t)\gamma^{XB}(\vec{r};\vec{R}_{FC}) \\
= \;& |\Psi^B_{nuc}(\vec{R}_{FC},t)|^2\triangle\rho^B(\vec{r};\vec{R}_{FC}) + 2Re\Psi^{X*}_{nuc}(\vec{R}_{FC},t)\Psi^B_{nuc}(\vec{R}_{FC},t)\gamma^{XB}(\vec{r};\vec{R}_{FC}),
\end{aligned}
$$

where $\triangle\rho^B(\vec{r};\vec{R}_{FC}) = \rho^B(\vec{r};\vec{R}_{FC}) - \rho^X(\vec{r};\vec{R}_{FC})$.

Time evolution of the excited differential electronic charge density at the FC geometry*

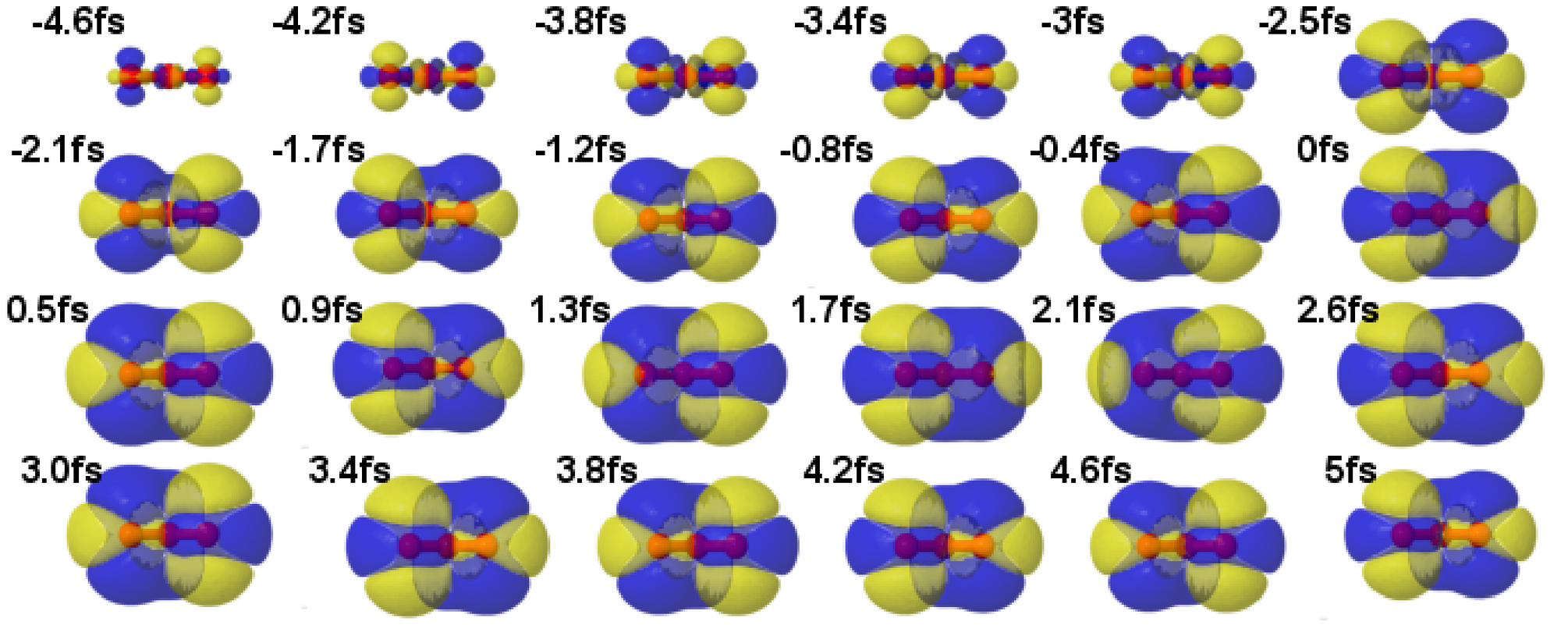

*G. J. Halász, A. Perveaux, B. Lasorne, M. A. Robb, F. Gatti and Á. V., PRA **88**, 023425 (2013).

- The electronic charge density oscillates from one bond to another with a period of 0.8 fs;

- The resulting electronic wave packet is thus a coherent superposition of two chemical structures, $O \cdots O_2$ and $O_2 \cdots O$;

- The subfemtosecond oscillation between both structures at the FC geometry prefigures that the dissociation of ozone could be controlled by modulating the electron density on the attosecond time scale;

Dyson Orbitals

The Dyson orbitals correspond to the molecular orbitals of the neutral molecule from which an electron has been removed where the cation relaxation is accounted for. They can be computed as one-electron transition amplitudes between the N-electron neutral and (N-1) -electron cationic states:

$$\Phi^{D}_{cat}(\vec{r};\vec{R}) = \sqrt{N}\int d\vec{r}_1 ... d\vec{r}_{N-1}\psi^{N}_{el,neut}(\vec{r}_1,...\vec{r}_N = \vec{r};\vec{R})\psi^{N-1}_{el,cat}(\vec{r}_1,...\vec{r}_{N-1};\vec{R}).$$

Time-dependent Dyson orbitals

These orbitals are useful when the neutral molecule is excited by an ultrashort laser pulse creating a coherent superposition of the different stationary states in the neutral molecule that will be probed in the next step by sudden XUV ionization

$$\begin{aligned}\Phi^{D}_{cat,i}(\vec{r};\vec{R},\tau) &= \sqrt{N}\int d\vec{r}_1 ... d\vec{r}_{N-1}\psi^{N}_{el,neut}(\vec{r}_1,...\vec{r}_N=\vec{r};\vec{R},\tau)\psi^{N-1}_{el,cat,i}(\vec{r}_1,...\vec{r}_{N-1};\vec{R}) \\ &= \sum_k \Psi^{k}_{nuc}(\vec{R},\tau)\Phi^{D}_{cat,i}(\vec{r};\vec{R});\end{aligned}$$

Here τ is the time when the ionization takes place and i denotes the different cation channels*.

*A. Perveaux, D. Lauvergnat, B. Lasorne, F. Gatti, M. A. Robb, G. J. Halász, and Á. Vibók: J. Phys. B. **47**, 124010 (2014).

At a given $\vec{R}$, $\psi^N_{el,neut}(\vec{r}_1, ...\vec{r}_N; \vec{R}, \tau)$ is the electronic wave packet, which is a coherent superposition of the ground (X) and the Hartley (B) states:

$$\psi^N_{el,neut}(\vec{r}_{el}; \vec{R}, \tau) = \Psi_{tot}(\vec{r}_{el}, \vec{R}, \tau) = \Psi^X_{nuc}(\vec{R}, \tau)\psi^X_{el}(\vec{r}_{el}; \vec{R}) + \Psi^B_{nuc}(\vec{R}, \tau)\psi^B_{el}(\vec{r}_{el}; \vec{R})$$

From this quantity the form of the time-dependent density of the Dyson orbitals at the FC geometry is:

$$\rho_{\Phi^D_{cat}}(\vec{r}; \vec{R}, \tau) = \sum_{k,l=X,B} \Psi^{k*}_{nuc}(\vec{R}, \tau)\Psi^{l}_{nuc}(\vec{R}, \tau)\Phi^{D,k*}_{cat}(\vec{r}; \vec{R})\Phi^{D,l}_{cat}(\vec{r}; \vec{R})$$

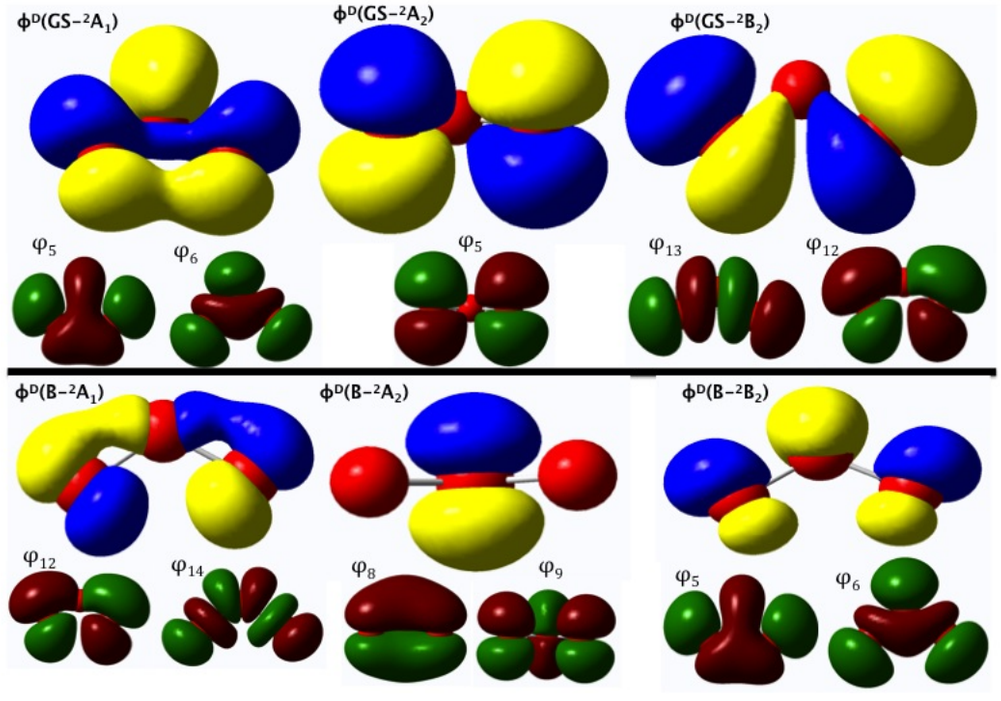

Time-independent Dyson orbitals between the two different electronic states (X, B) of the neutral and the three different channels ($^2A_1$, $^2B_2$ and $^2A_2$) of the cation. The most important molecular orbital components of the Dyson orbitals are also shown.

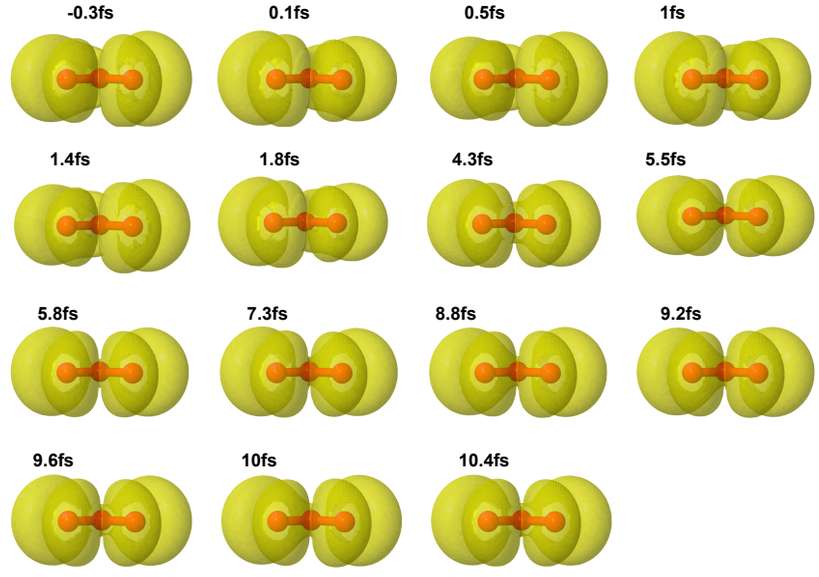

Time-dependent densities of the Dyson orbitals belong to $^2B_2$ cation channel

Attosecond photoelectron spectroscopy

Question arises whether photoionization from X or B could ever be discriminated when using an XUV attosecond probe pulse with a large bandwidth?

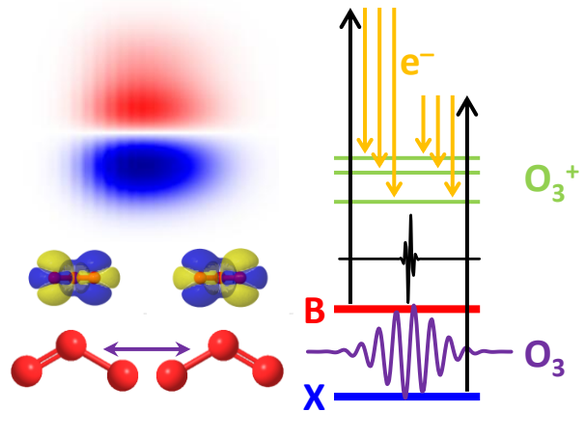

We believe the answer is yes, and **attosecond photoelectron spectroscopy** can be used to monitor the creation of an electronic wavepacket*.

*A. Perveaux, D. Lauvergnat, F. Gatti, G. J. Halász, Á. Vibók and B. Lasorne: J. Phys. Chem. A. DOI: 10.1021/jp508218n (2014).

- Many ionic channels can be accessed upon photoionising from either X or B, and a number of transitions will overlap within the same energy window;

- The bandwidth of the attosecond probe will be large: a few eV for a few-hundred-as pulse;

- This may prevent any characteristic feature in the spectrum to be observed;

- Preliminary numerical simulations are thus essential for future experiments in order to prove first that contributions from X or B will indeed be discriminated over time and to identify which energy window is adequate to do so;

- Using accurate quantum dynamics and quantum chemistry calculations, we generated the time-resolved photoelectron spectrum (TRPES);

Photoionization Spectrum

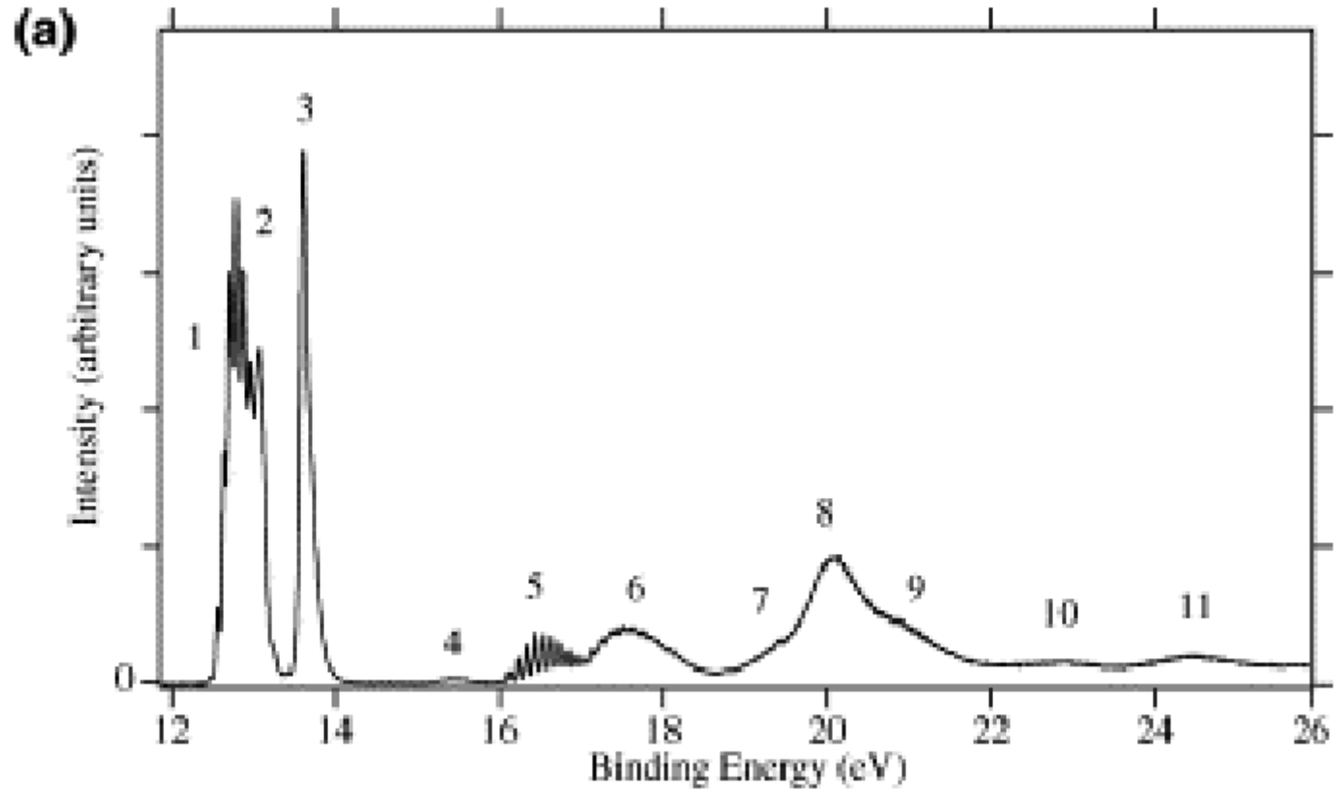

Experimental photoionization spectrum from X state (CPL 375, 76 (2003)).

Ab initio energy differences (MRCI/cc-pVDZ level of theory) with respect to X and B states at the FC point (B is 5.8 eV above X). We consider 19 states of the cation.

Cation states (j)	$E_j - E_X/eV$	$E_j - E_B/eV$
$1(1^2A_1)$	12.38	6.59
$2(1^2B_2)$	12.51	6.72
$3(1^2A_2)$	13.20	7.42
$4(1^2B_1)$	14.15	8.36
$5(2^2A_2)$	14.45	8.66
$6(2^2B_2)$	15.18	9.40
$7(2^2A_1)$	15.58	9.80
$8(2^2B_1)$	16.35	10.56
$9(3^2A_2)$	16.50	10.72
$10(3^2B_1)$	17.10	11.32
$11(3^2A_1)$	17.32	11.54
$12(3^2B_2)$	17.65	11.87
$13(4^2B_2)$	18.19	12.41
$14(4^2A_2)$	18.63	12.85
$15(4^2B_1)$	18.61	12.83
$16(4^2A_1)$	19.07	13.29
$17(5^2B_2)$	19.61	13.83
$18(5^2A_1)$	19.49	13.70
$19(6^2B_2)$	19.94	14.16

Assuming “atomic” picture (the rovibrational dynamics and its influence on the structure of the spectrum are ignored), the energy resolved PES appear as stick spectra with lines approximately centered at the vertical energy differences:

$$I_k(\varepsilon) = \sum_j I_{jk}\delta(\varepsilon - \varepsilon_{jk}).$$

Dyson norms ($I_{jk} = \left\langle \Phi_{j,k}^{Dyson} | \Phi_{j,k}^{Dyson} \right\rangle$) are good predictors of the corresponding ionization yields, they give the relative intensities of the corresponding peaks.

(PRA, 86, 053406, 2012)

Dyson norms

State Pairs	Dyson norms	State Pairs	Dyson norms
Neutral X-Cation 1	0.60	Neutral B-Cation 1	0.05
Neutral X-Cation 2	0.45	Neutral B-Cation 2	0.07
Neutral X-Cation 3	0.63	Neutral B-Cation 3	0.03
Neutral X-Cation 4	0.00	Neutral B-Cation 4	0.00
Neutral X-Cation 5	0.00	Neutral B-Cation 5	0.00
Neutral X-Cation 6	0.01	Neutral B-Cation 6	0.07
Neutral X-Cation 7	0.00	Neutral B-Cation 7	0.05
Neutral X-Cation 8	0.19	Neutral B-Cation 8	0.36
Neutral X-Cation 9	0.00	Neutral B-Cation 9	0.00
Neutral X-Cation 10	0.08	Neutral B-Cation 10	0.07
Neutral X-Cation 11	0.20	Neutral B-Cation 11	0.25
Neutral X-Cation 12	0.04	Neutral B-Cation 12	0.23
Neutral X-Cation 13	0.01	Neutral B-Cation 13	0.03
Neutral X-Cation 14	0.00	Neutral B-Cation 14	0.00
Neutral X-Cation 15	0.00	Neutral B-Cation 15	0.00
Neutral X-Cation 16	0.00	Neutral B-Cation 16	0.01
Neutral X-Cation 17	0.03	Neutral B-Cation 17	0.08
Neutral X-Cation 18	0.22	Neutral B-Cation 18	0.08
Neutral X-Cation 19	0.19	Neutral B-Cation 19	0.02

Stick PES from X(blue) or B(red) as functions the KER for a probe photon at 95 eV.

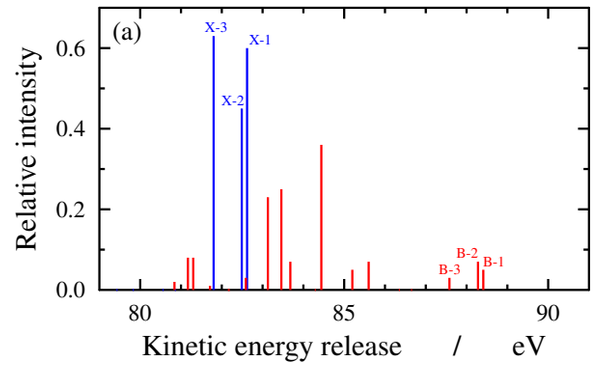

This stick spectra can be convoluted with a Gaussian window function to mimic the width due to the bandwidth of the XUV photoionising probe pulse. (For the parameters obtained from the experiment $\sigma = 1.5$ eV (in energy domain)).

The energy-resolved spectra are approximated as:

$$I_k(\varepsilon) = \frac{1}{\sigma\sqrt{2\pi}} \sum_j e^{-\frac{(\varepsilon-\varepsilon_{jk})^2}{2\sigma^2}} I_{jk},$$

where the KER of the electron is:

$$\epsilon_{jk} = E_k + E_{photon} - E_j.$$

The spectral distribution of the probe pulse is ignored and the probe energy is:

$$E_{photon} = 95\text{eV}.$$

Convoluted PES from X(blue) and B(red) as function the KER for $E_{photon} = 95$eV

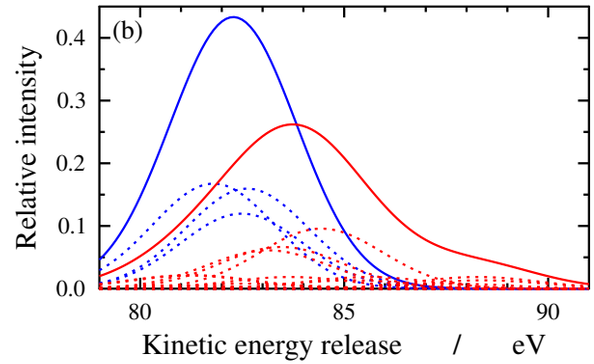

The time evolution of the molecular wave packet is:

$$\left|\psi_{mol}(\vec{R},t)\right\rangle = \sum_{k=X,B} \psi_{nuc}^{(k)}(\vec{R},t) \left|\psi_{el}^{(k)};\vec{R}\right\rangle .$$

The effective electronic wave packet at the FC point ($\vec{R} = \vec{R}_{FC}$) is:

$$|\psi_{el}(t)\rangle = \sum_{k=X,B} c_k(t) \left|\psi_{el}^{(k)};\vec{R}_{FC}\right\rangle .$$

Here $|\psi_k\rangle$ are the adiabatic electronic states of the neutral molecule at FC point and $c_k(t)$ are the renormalized nuclear wave packet components at the FC point:

$$c_k(t) = \psi_{nuc}^{(k)}(\vec{R}_{FC},t) / \sqrt{\sum_{l=X,B} \left|\psi_{nuc}^{(l)}(\vec{R}_{FC},t)\right|^2}.$$

The local populations and coherences at the FC point are:

$$\rho_{kk,}(t) = c_k^*(t)c_k,(t) = \frac{\psi_{nuc}^{(k)*}(\vec{R}_{FC},t)\psi_{nuc}^{(k,)}(\vec{R}_{FC},t)}{\sum_{l=X,B}\left|\psi_{nuc}^{(l)}(\vec{R}_{FC},t)^2\right|^2}.$$

For a stick spectrum, the intensity as a function of the time delay can be approximated as (for each cation channel):

$$I_j(\tau) = \sum_{k=X,B}\rho_{kk}(\tau)I_{jk}.$$

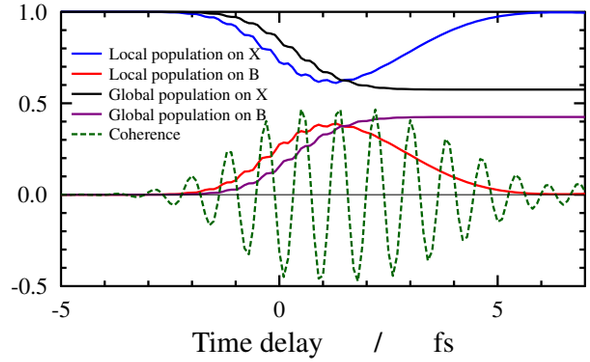

Local X (blue) and B (red) populations and coherence (green; real part) at the FC point as functions of time (origin coincident with the maximum of the pump pulse). Global X (black) and B (purple) populations ($P_k(t) = \int \rho_{kk}(\overrightarrow{R}, \overrightarrow{R}, t) d\overrightarrow{R}$) as functions of time).

Using the same convolution procedure as above leads to the **time-resolved PES**

$$I(\varepsilon,\tau) = \sum_{k=X,B} \rho_{kk}(\tau) I_{jk} = \frac{1}{\sigma\sqrt{2\pi}} \sum_{k=X,B} \rho_{kk}(\tau) \sum_j e^{-\frac{(\varepsilon-\varepsilon_{jk})^2}{2\sigma^2}} I_{jk}$$

Approximate PES as a function of the time delay(horizontal axis) and KER(vertical axis)

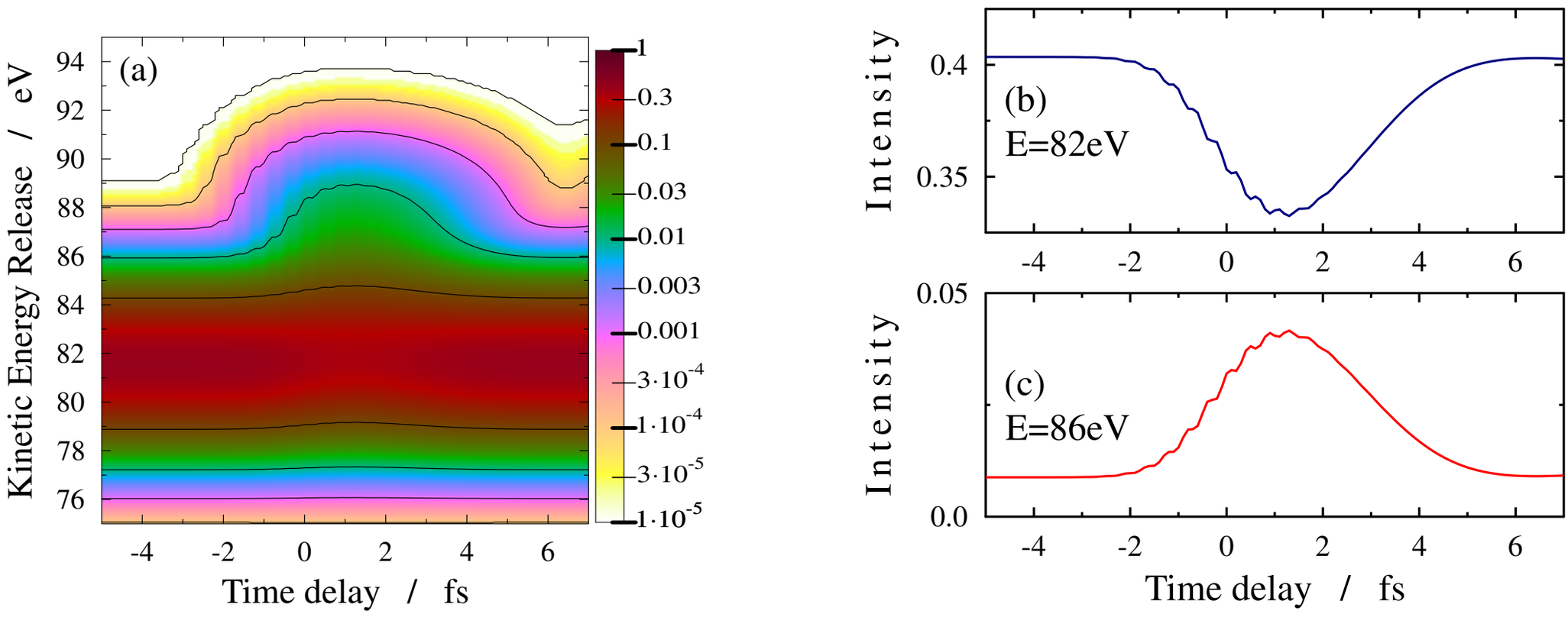

Panel a: approximate TRPES (logarithmic scale) as a function of the time delay (horizontal axis) and kinetic energy release (vertical axis); panel b: cut at 82 eV (linear scale); panel c: cut at 86 eV (linear scale).

Two significant effects can be noticed:

- *i)* around 82 eV (panel b), between $\tau = 0$ and 3 fs – while the pump pulse is still on – the intensity decreases to 0.33, in contrast with its value of 0.40 for $\tau < 0$ or > 3 fs;

- *ii)* around 86 eV (panel c) the intensity increases from 0.01 to 0.04 and returns to 0.01 during the same delay time intervals.

- Better contrast is obtained by considering the differential TRPES obtained by removing the contribution from pure X at all times;

Approximate differential TRPES as a function of the time delay and kinetic energy release

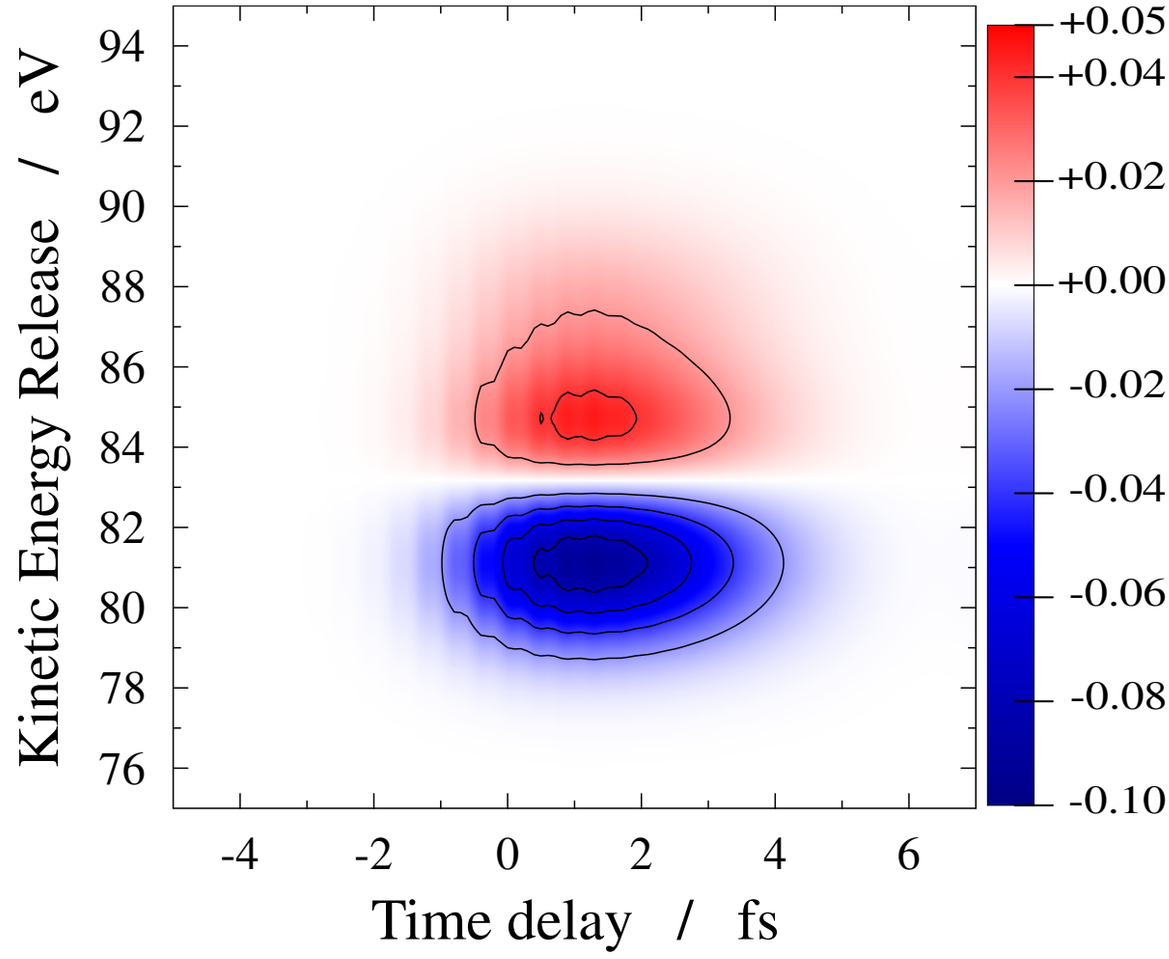

- The central objective was to determine with numerical simulations if TRPES experiments will be able to monitor the generation of an electronic wavepacket in the ozone molecule on its real time scale.

- Observing the electronic motion in the neutral before any significant nuclear motion requires using a few-femtosecond UV pulse as a pump.

- It is shown that two energy regions can be distinguished: one exhibiting depletion of X and one where production of B is specifically observed in two distinct energy regions, despite a large bandwidth and overlapping channels.

Quantum control by laser-induced conical intersections

Strong Field Control

It uses non-perturbative fields which too week to ionise a molecule, but strong enough to shape the PESs through the Stark effect.

Non-resonant dynamic Stark effect (**NRDSE**): shifting of energy levels by a field which is off-resonance with any vibrational and electronic transitions;

Resonant dynamic Stark effect (**RDSE**): shifting of energy levels by a field which is resonance with any vibrational and electronic transitions (population transfer!);

- It is well known that **Conical Intersections (CIs) cannot be formed** in field-free diatomics.

- **But**, by applying external electric fields, CIs can be created even in diatomics.

- In this situation the **laser light induces CIs (LICIs)** which **couple** the **electronic states** and the internal **rotational** and **vibrational** motions.

- The **LICI** is a **RDSE** and the control is derived from **resonant dipole interactions**.

The Hamiltonian of a diatomic molecule in a linearly polarized laser wave given by formula

$$\mathbf{H}(t) = \widehat{T}_{R,\Theta,\Phi} + \mathbf{H}_{el}(R) + \varepsilon_0 \cos(\omega_L t) \sum_j (z_j \cos\Theta + x_j \sin\Theta)$$

The ω_L laser frequency can couple two electronic states ($|\psi_1^e>, |\psi_2^e>$) of the molecule by single photon excitation.

For the case of Na_2 molecule ($X^1\sum_g^+$and $A^1\sum_g^+$, $\lambda = 667nm$).

Due to symmetry, the only non-vanishing dipole matrix element responsible for light-induced electronic transitions is $d(R) =< \psi_1^e| \sum_j z_j |\psi_2^e >$.

N. Moiseyev, M. Sindelka and L.S. Cederbaum, *J. Phys. B*: 41 (2008) 221001.
M. Sindelka, N. Moiseyev and L.S. Cederbaum, *J. Phys. B*: 44 (2011) 045603.

In the space of the two electronic states the static, dressed state representation (Floquet representation) form of this Hamiltonian is the following:

$$\mathbf{H} = \left(-\frac{\hbar^2}{2\mu}\frac{\partial^2}{\partial R^2} + \frac{\mathbf{L}^2_{\theta\varphi}}{2\mu R^2} \right) \otimes \begin{pmatrix} 1 & 0 \\ 0 & 1 \end{pmatrix} + \begin{pmatrix} V_X(R) & (\mathcal{E}_0/2)\, d(R)\, \cos\theta \\ (\mathcal{E}_0/2)\, d(R)\, \cos\theta & V_A(R) - \hbar\omega_L \end{pmatrix}$$

Let us diagonalize the potential matrix to obtain the two adiabatic (BO) PES ($V_{ad}^{lower}(R,\theta); V_{ad}^{upper}(R,\theta)$). One can obtain CI only if the **two conditions** $\cos\theta = 0, (\theta = \pi/2)$ and $V_X(R) = V_A(R) - \hbar\omega_L$ are simultaneously fulfilled.

The laser induced CI leads to a breakdown of the B-O picture of single surface dynamics.

Let us diagonalize the potential matrix and thus transform $\hat{H}$ to the adiabatic representation:

$$\widehat{U}(R,\theta) = \begin{pmatrix} \cos\Phi(R,\theta) & \sin\Phi(R,\theta) \\ -\sin\Phi(R,\theta) & \cos\Phi(R,\theta) \end{pmatrix}$$

where

$$\Phi(R,\theta) = \tfrac{1}{2}\arctan\left(\frac{\varepsilon_0\, d(R)\,\cos\theta}{E_A(R)-\hbar\omega_L-E_X(R)}\right).$$

In this representation $\hat{U}\hat{H}\hat{U}^{\dagger}$ gives the **adiabatic** PES ($V_{ad}^{upper}(R,\theta); V_{ad}^{lower}(R,\theta)$) and the kinetic energy operator contains the nonadiabatic couplings.

Light-induced CIs introduce infinitely strong nonadiabatic coupling!

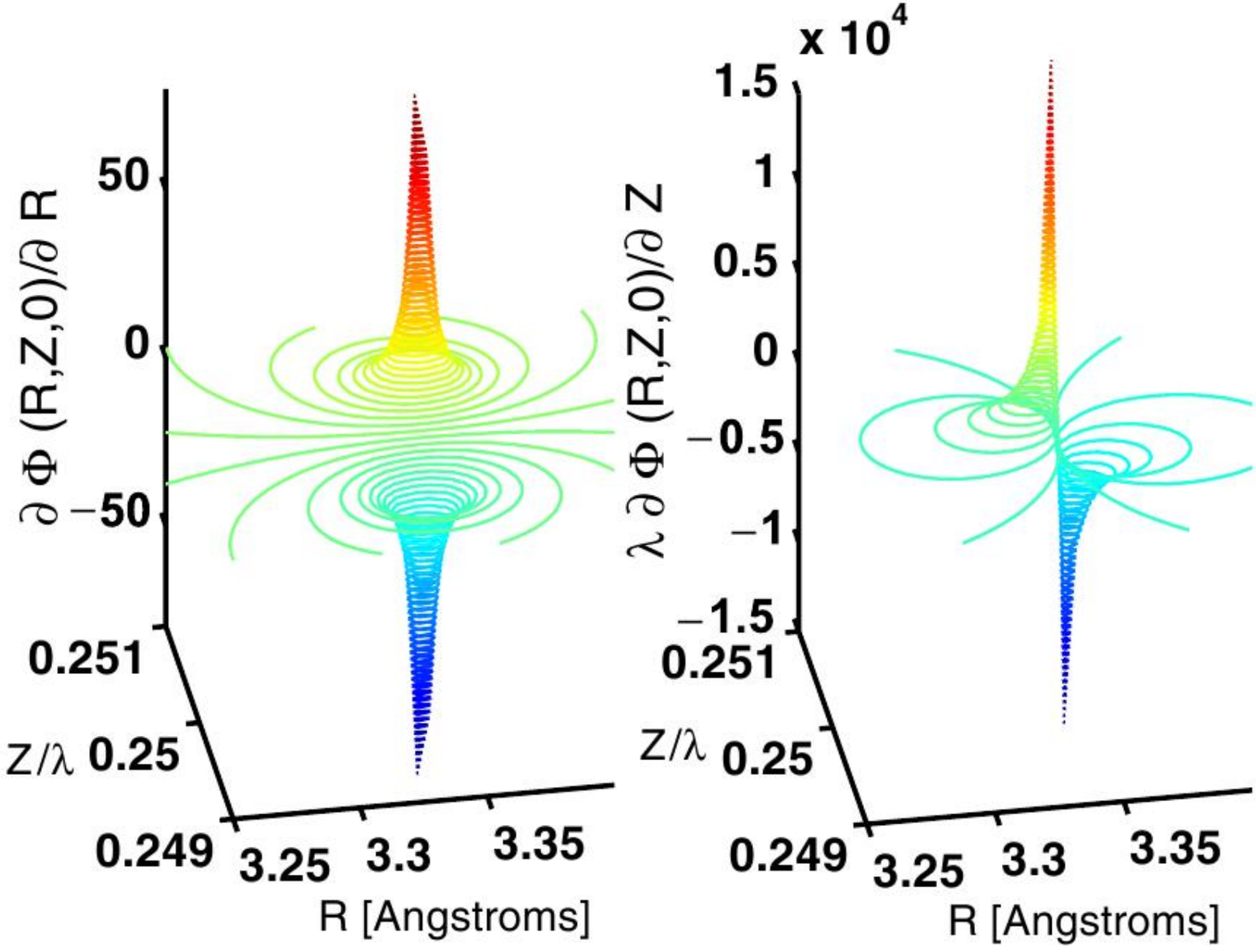

Topological or Berry phase (BF)

- It is known that each real adiabatic electronic state **changes sign** when transported continuously along a closed loop enclosing the point of CI.

- As the total wave function must be single valued one has to multiply it by a phase factor ensuring that the total wave function remains **single valued**.

- This modification has a **direct effect** on the nuclear dynamics.

- Consequently, the **appearance of the BF** in a molecular system can be considered as a **clear signature of the CI** independently of whether it is natural or a laser induced one.

G. Herzberg and H.C. Longuet-Higgins, *Diss. Faraday. Soc:* 35 (1963) 77.
M. V. Berry: *Proc. R. Soc. A*: 392 (1984) 45.

It is known that the topological or BF α_{12} can be calculated for a closed contour Γ as

$$\alpha_{12} = \oint_{\Gamma} \tau_{12}(s') \cdot ds',$$

where τ_{12} is the nonadiabatic coupling term between the two electronic states.

It is also known that*

$$\alpha_{12} = \pi \begin{cases} 2n+1 & \Gamma \; encircles \; odd \; number \; of \; CIs \\ 2n & \Gamma \; encircles \; even \; number \; of \; CIs \end{cases} \quad n = 0, \pm 1, \pm 2, ...$$

In our case it is easy to see that:

$$\alpha_{12} = \Phi_{end}(R, \Theta) - \Phi_{begin}(R, \Theta).$$

M. Baer, *Chem. Phys. Lett*. 35 (1975) 112; M. Baer, A. Alijah, *Chem. Phys. Lett*. 319 (2000) 489; M. Baer, *Chem. Phys*. 259 (2000) 123.

*These are the consequences that each adiabatic state chages sign when transported continuously along a closed loop enclosing the point of intersection.

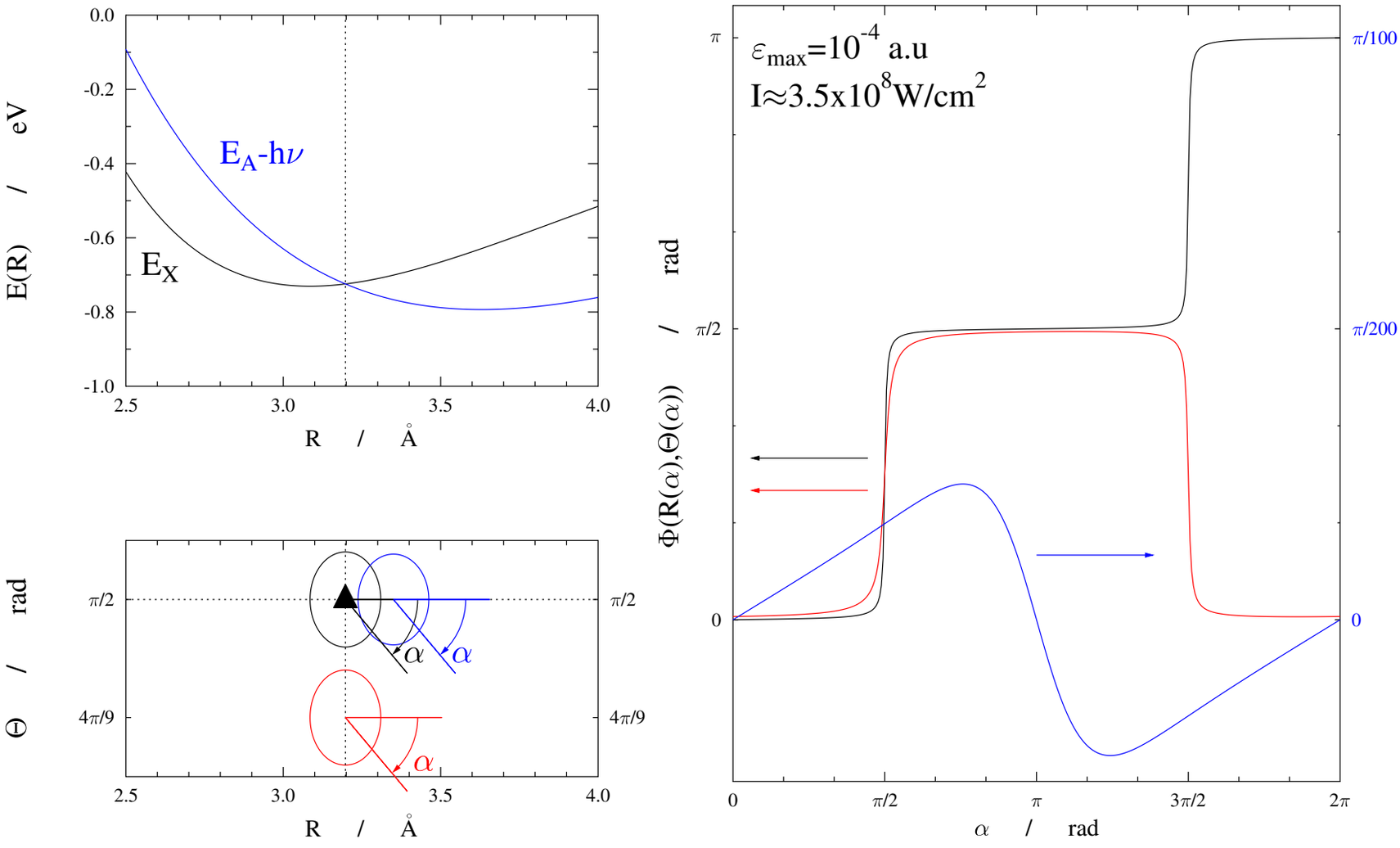

G. J. Halász, Á. Vibók, M. Sindelka, N. Moiseyev and L.S. Cederbaum, *J. Phys. B*: **44**, 175102, (2011).

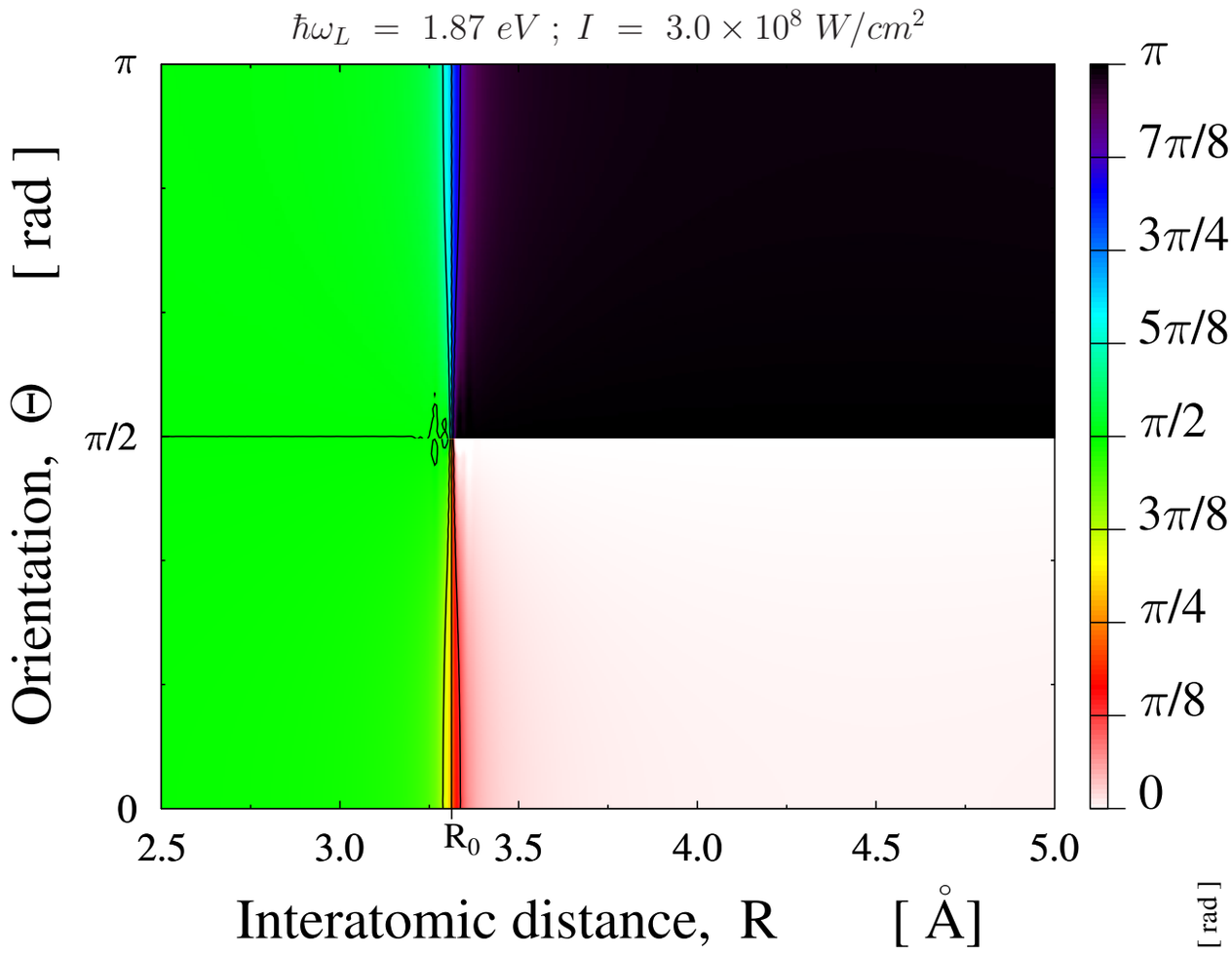

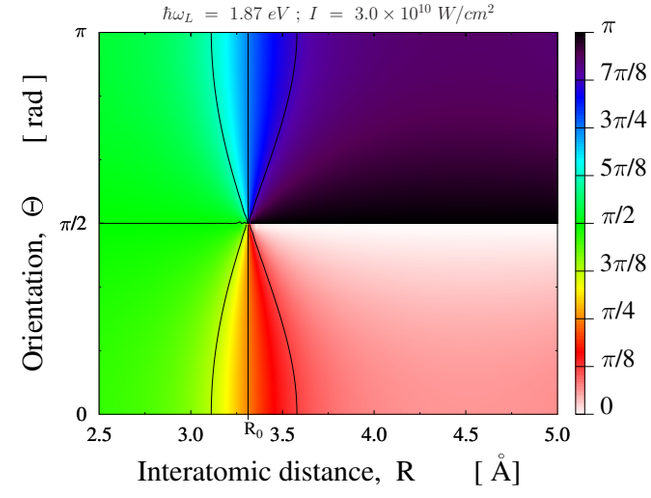

G.

J. Halász, Á. Vibók, M. Sindelka, N. Moiseyev and L.S. Cederbaum, *J. Phys. B.*: **44**, 175102, (2011).

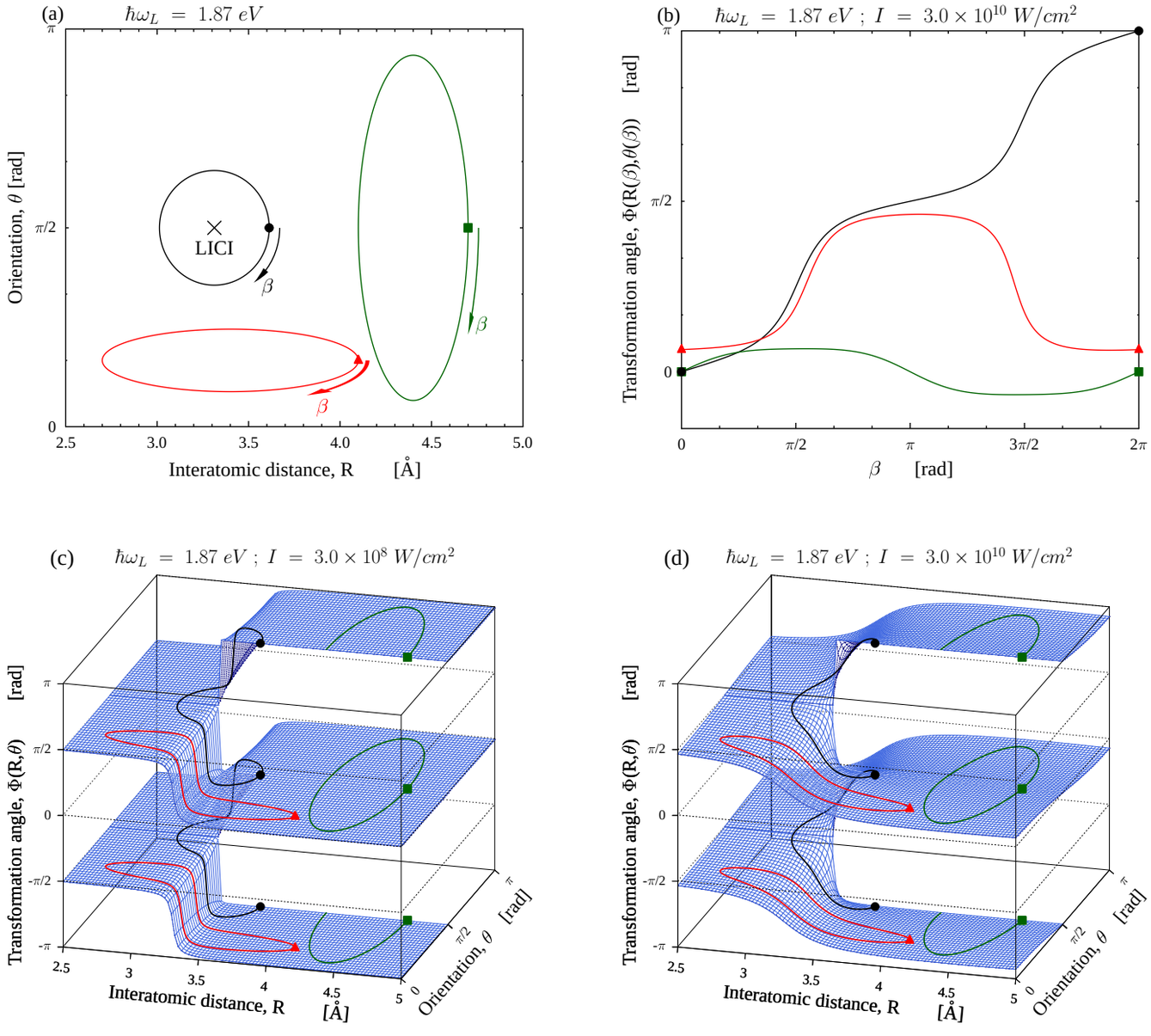

G. J. Halász, M. Sindelka, N. Moiseyev, L.S. Cederbaum and Á. Vibók, *J. Chem. Phys. A.*: **116**, 2636, (2012).

Wave packet dynamics

One has to solve the time-dependent nuclear Schrödinger-equation which is the following:

$$i\hbar\frac{\partial}{\partial t}|\psi(R,\theta,t)>=\widehat{H}\,|\psi(R,\theta,t)>$$

$$|\psi(R,\theta,t)>=\exp(\tfrac{i}{\hbar}\,\widehat{H}\,t)|\psi(R,\theta,0)>$$

The initial wave function is chosen as the electronic and rovibrational ground state solution of the field free Hamiltonian:

$$|\psi(R,\theta,t=0)>=(|\varphi^{X}_{\nu=0,\,J=0}(R,\theta)>;0)^{T}$$

Calculated dynamical quantities

The autocorrelation function gives the overlap between the initial and the time evolved nuclear wave packets:

$$\begin{aligned} C(t) &= |<\psi(R,\theta,0)|\psi(R,\theta,t)>| \\ &= \left|\int_0^{\pi} d\theta \cdot \sin\theta \int_0^{\infty} dR \cdot \psi(R,\theta,0)^* \cdot \psi(R,\theta,t)\right|. \end{aligned}$$

The diabatic population $P^A(t)$ on the excited A surface (or probability of being on the excited A state diabatic surface) is:

$$\begin{aligned} P^A(t) &= <\psi^A(R,\theta,t)|\psi^A(R,\theta,t)>= \\ &\int_0^{\pi} d\theta \cdot \sin\theta \int_0^{\infty} dR \cdot \psi^A(R,\theta,t)^* \cdot \psi^A(R,\theta,t). \end{aligned}$$

The degree of the molecular alignment as a function of time is:

$$<\cos^2\theta>=<\psi(R,\theta,t)|\cos^2\theta|\psi(R,\theta,t)> .$$

G. J. Halász, M. Sindelka, N. Moiseyev, L.S. Cederbaum and Á. Vibók, *J. Chem. Phys. A.*: **116**, 2636, (2012).

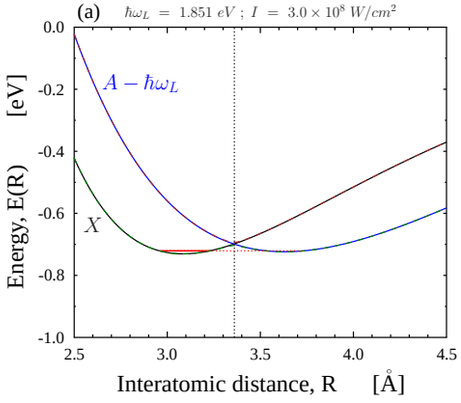

(a) Potential energy X and field-dressed potential energy $A-\hbar\omega_L$ curves of Na_2. The dashed-dotted vertical line indicates the geometric position of the CI and the dashed-dotted horizontal line the energy position of the initial state of the propagation.

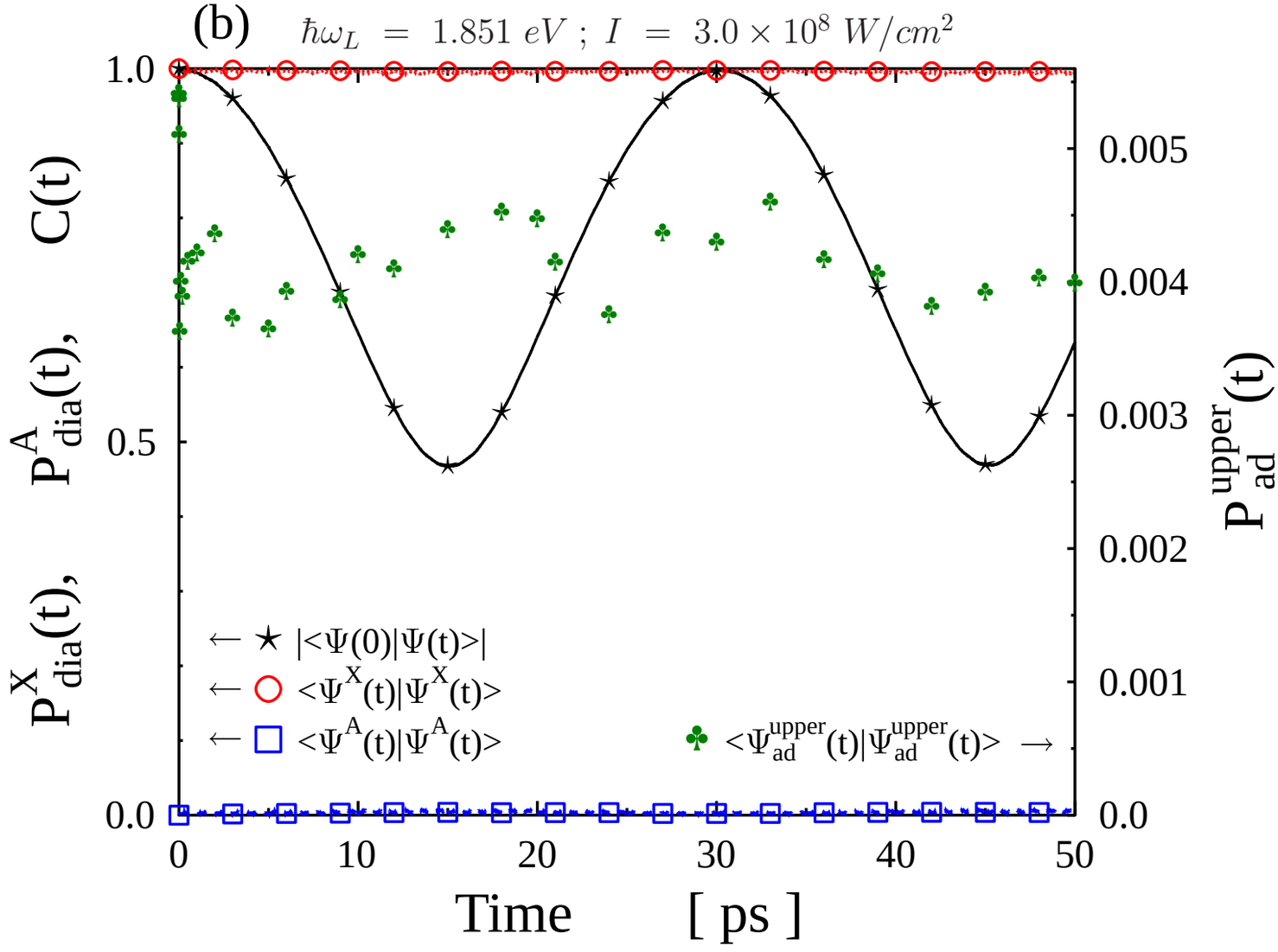

(b) Autocorrelation function (⋆ ⋆ ⋆⋆), population on the ground state diabatic surface (○ ○ ○○), on the excited state diabatic surface (□□□□) and on the adiabatic upper state surface (♣♣♣♣) are shown as a function of time.

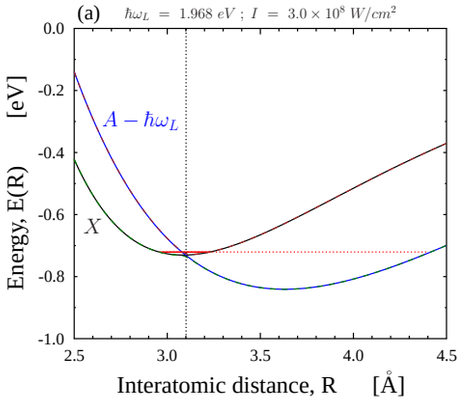

(a) Potential energy X and field-dressed potential energy $A-\hbar\omega_L$ curves of Na_2. The dashed-dotted vertical line indicates the geometric position of the CI and the dashed-dotted horizontal line the energy position of the initial state of the propagation.

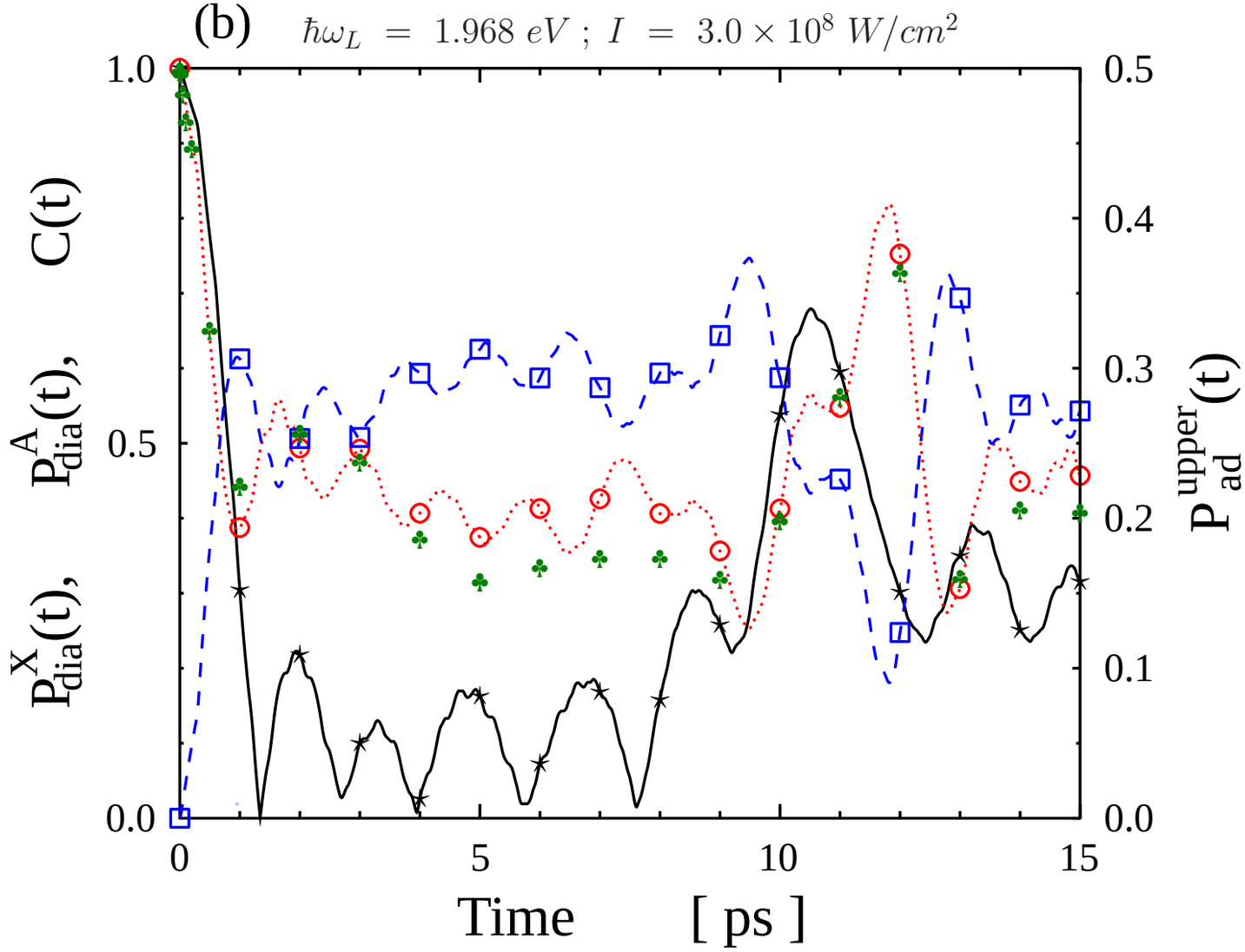

(b) Autocorrelation function (⋆ ⋆ ⋆⋆), population on the ground state diabatic surface (○ ○ ○○), on the excited state diabatic surface (□□□□) and on the adiabatic upper state surface (♣♣♣♣) are shown as a function of time.

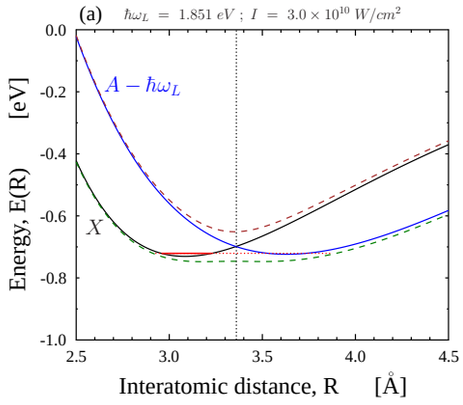

(a) Potential energy X and field-dressed potential energy $A-\hbar\omega_L$ curves of Na_2. Shown are also the respective adiabatic potential curves at $\theta = 0$ as dashed curves. The dashed-dotted vertical line indicates the geometric position of the CI and the dashed-dotted horizontal line the energy position of the initial state of the propagation.

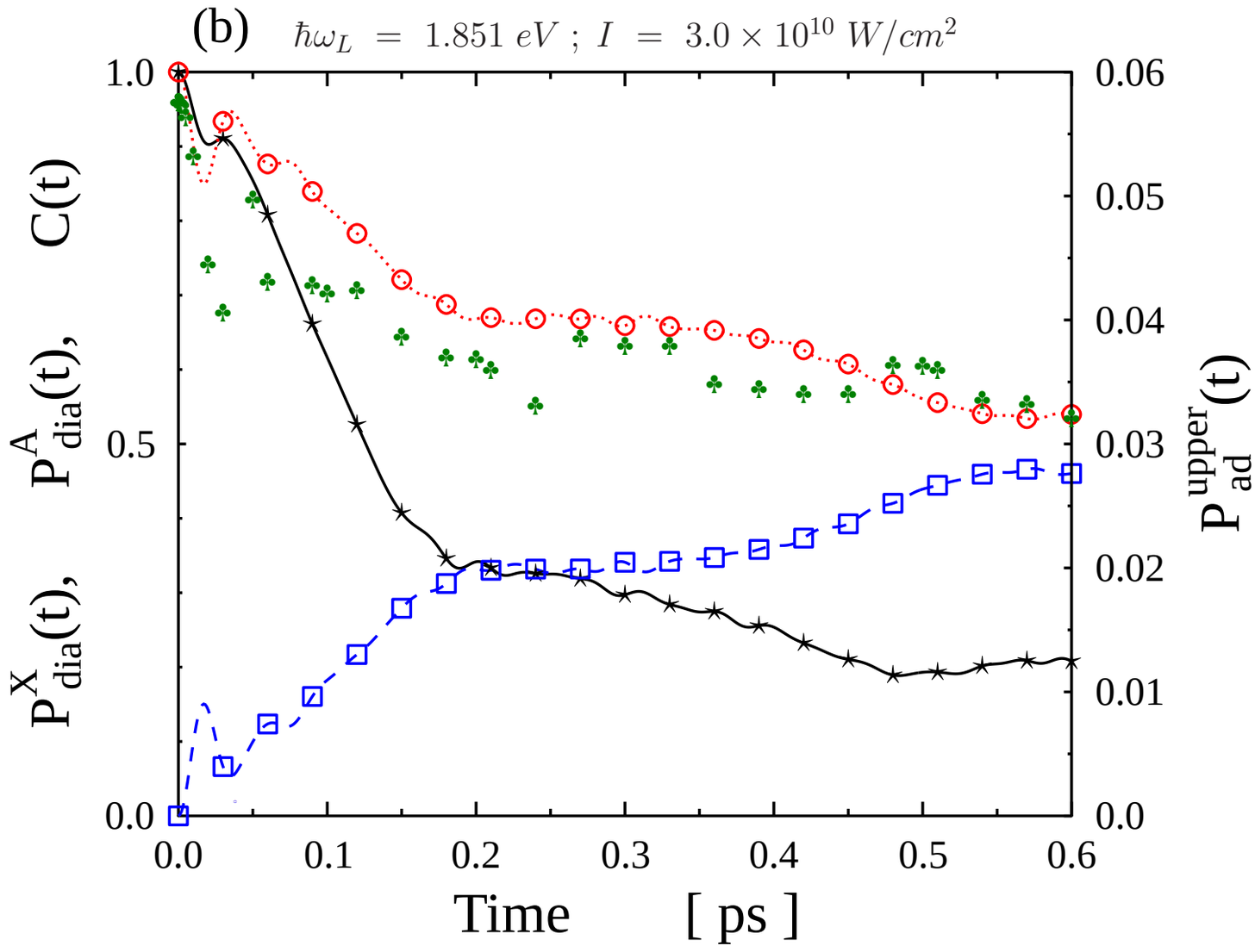

(b) Autocorrelation function ($\star\star\star\star$), population on the ground state diabatic surface ($\circ\circ\circ\circ$), on the excited state diabatic surface ($\square\square\square\square$) and on the adiabatic upper state surface ($\clubsuit\clubsuit\clubsuit\clubsuit$) are shown as a function of time.

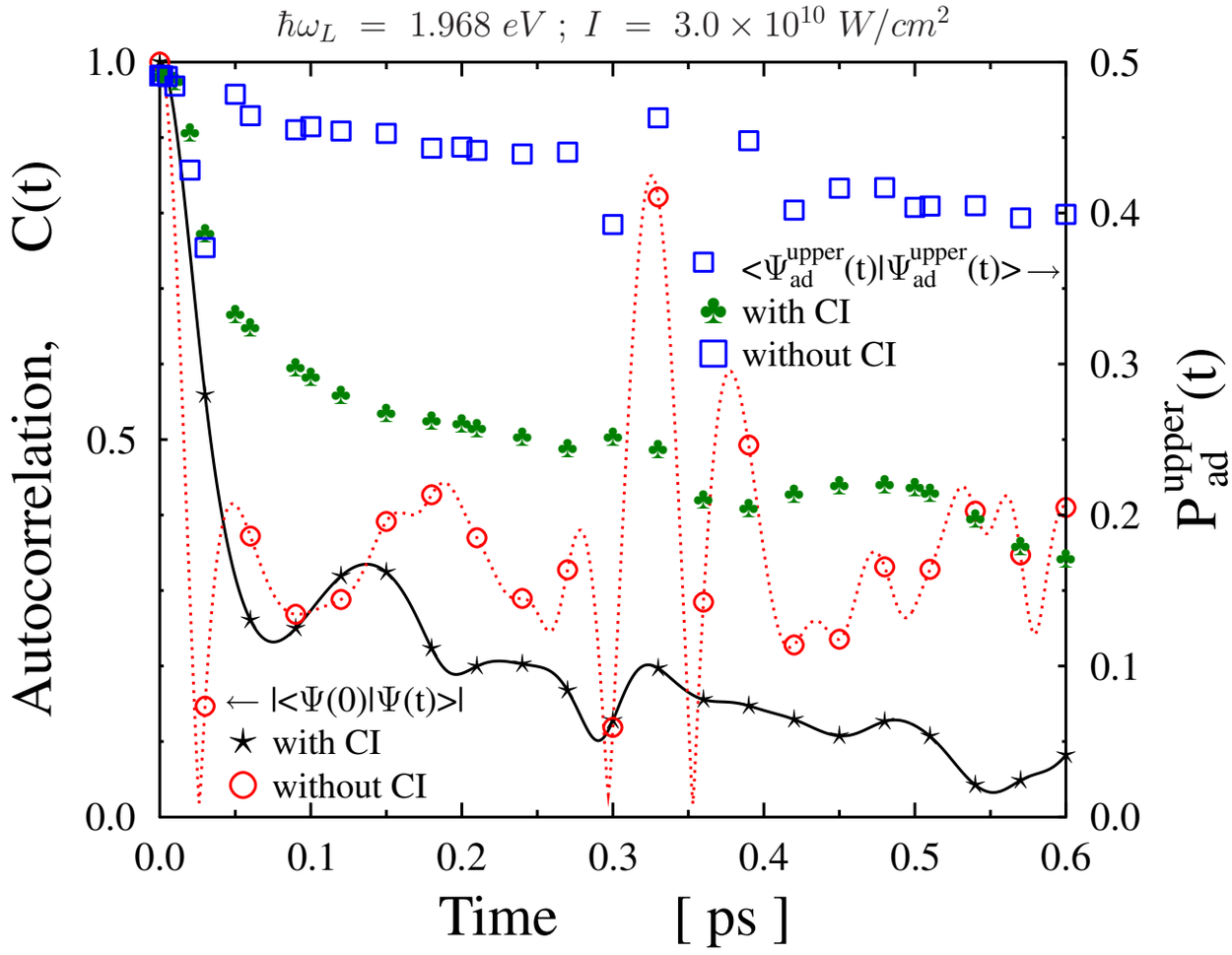

Autocorrelation function and population on the adiabatic upper state surface as a function of time for the "no CI" case where the rotational motion has been frozen ($\cos\theta = 1$). The results are compared with those of the full calculations ("CI" case). The laser field intensity and photon energy are: $I = 3.0 \times 10^{10} \frac{W}{cm^2}$ and $\hbar\omega_L = 1.968\, eV$. The curves of the autocorrelation function are marked with ($\star\star\star\star$) and ($\circ\circ\circ\circ$) for the "CI" and "no CI" cases, respectively. The curves of the upper state population are marked with ($\clubsuit\clubsuit\clubsuit\clubsuit$) and ($\square\square\square\square$) for the "CI" and "no CI" cases, respectively.

Molecular alignment

- Sufficiently intense laser pulse makes possible to perform strongly aligned angular distribution of a gas-phase molecular sample.

- In this case, still in the gas phase, the molecules are oriented in space with their axes along the polarization vector of the laser.

- If no permanent dipole moment, this effect is mediated by the interaction of the electric field of the laser with the induced dipole in the molecule.

G. J. Halász, Á. Vibók, M. Šindelka, L. S. Cederbaum and N. Moiseyev: *Chem. Phys.* **399**, 146, (2012).

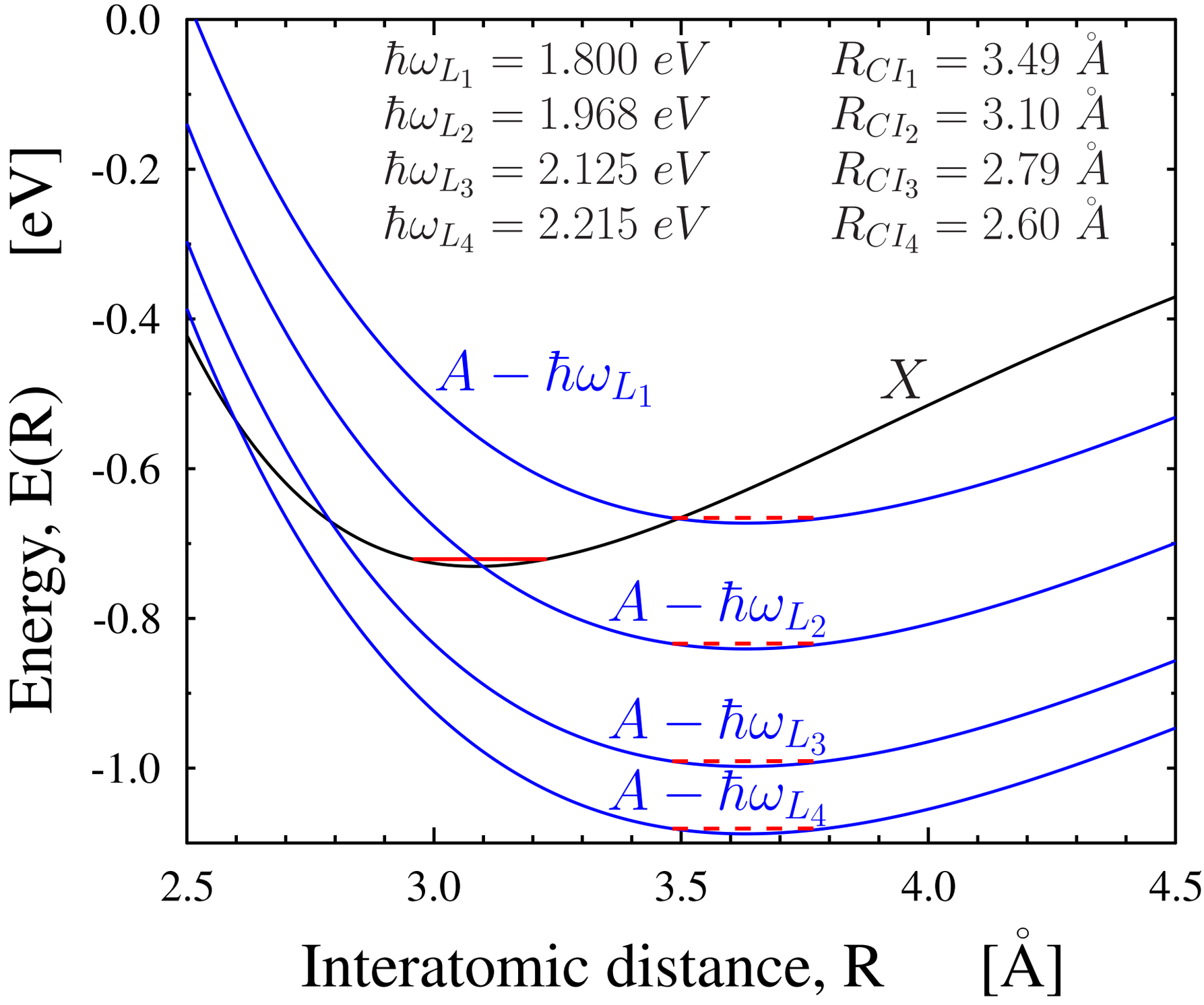
$\hbar\omega_{L_1} = 1.800\ eV$
$\hbar\omega_{L_2} = 1.968\ eV$
$\hbar\omega_{L_3} = 2.125\ eV$
$\hbar\omega_{L_4} = 2.215\ eV$
$R_{CI_1} = 3.49\ \mathring{A}$
$R_{CI_2} = 3.10\ \mathring{A}$
$R_{CI_3} = 2.79\ \mathring{A}$
$R_{CI_4} = 2.60\ \mathring{A}$
$A - \hbar\omega_{L_1}$
X
$A - \hbar\omega_{L_2}$
$A - \hbar\omega_{L_3}$
$A - \hbar\omega_{L_4}$
0.0
-0.2
-0.4
-0.6
-0.8
-1.0
Energy, E(R) [eV]
2.5
3.0
3.5
4.0
4.5
Interatomic distance, R [Å]

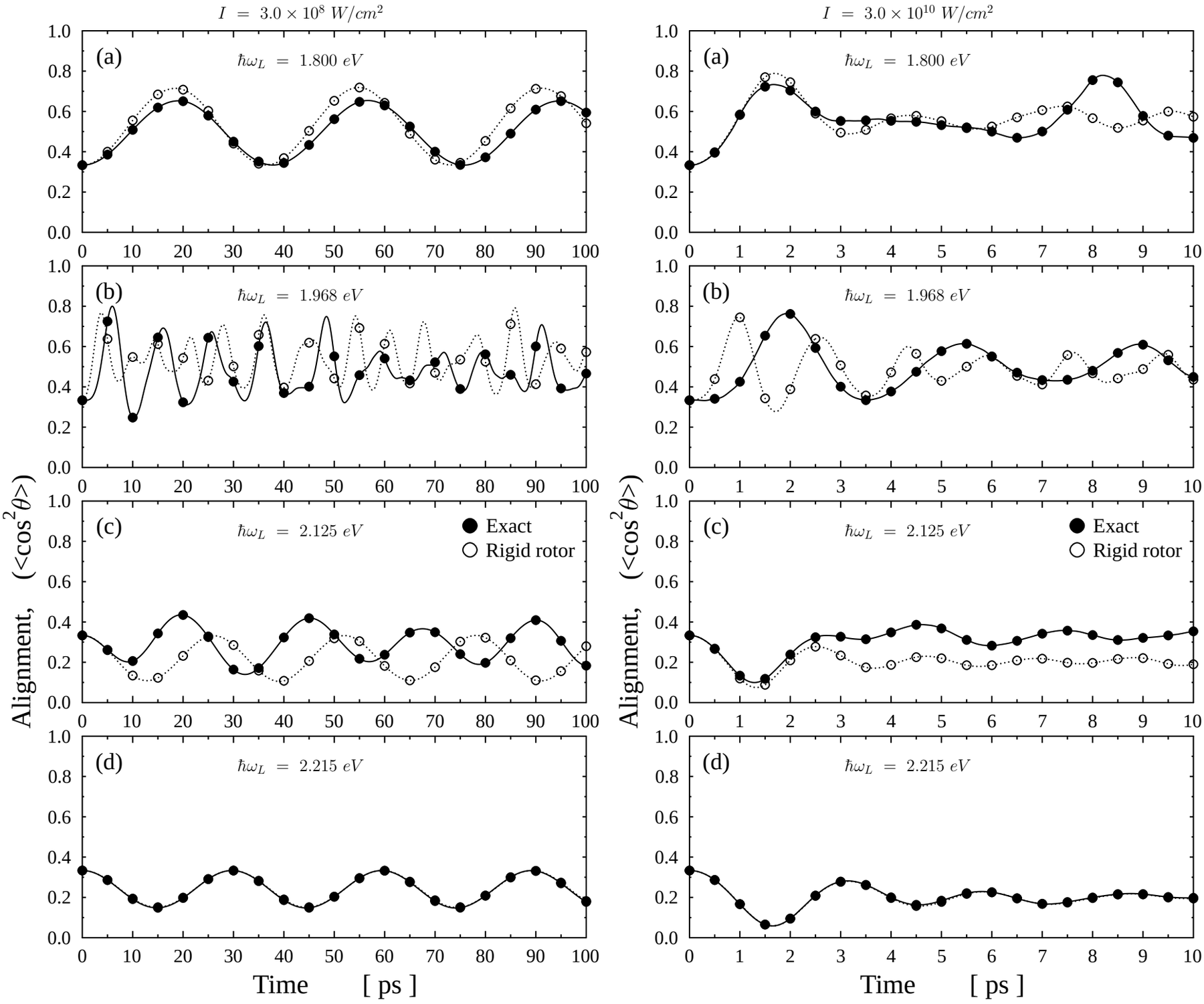
$I = 3.0 \times 10^8\ W/cm^2$
$I = 3.0 \times 10^{10}\ W/cm^2$
(a)
(b)
(c)
(d)
$\hbar\omega_L = 1.800\ eV$
$\hbar\omega_L = 1.968\ eV$
$\hbar\omega_L = 2.125\ eV$
$\hbar\omega_L = 2.215\ eV$
Exact
Rigid rotor
Alignment, ($<\cos^2\theta>$)
Time [ps]

- So far the Floquet representation was used to describe the nuclear Hamiltonian;

- This representation is very illustrative and helps to understand the essence of the light-induced nonadiabatic effect;

- The question arises: what are the limits of the Floquet approximation?

The 2x2 Floquet Hamiltonian is:

$$\hat{\mathbf{H}} = \begin{pmatrix} -\frac{\hbar^2}{2\mu}\frac{\partial^2}{\partial R^2} + \frac{L^2_{\theta\varphi}}{2\mu R^2} & 0 \\ 0 & -\frac{\hbar^2}{2\mu}\frac{\partial^2}{\partial R^2} + \frac{L^2_{\theta\varphi}}{2\mu R^2} \end{pmatrix} + \begin{pmatrix} V_X & (\epsilon_0/2)d(R)\cos\theta \\ (\epsilon_0/2)d(R)\cos\theta & V_A - \hbar\omega_L \end{pmatrix};$$

Let us start from the time-dependent Schrödinger equation that one needs to solve to describe the dynamics

$$i\dot{\Psi}(t) = \hat{H}(t)\Psi(t) = \left[\hat{T}_{nuc} + \hat{H}_{el} + \hat{d}\cdot E(t)\right]\Psi(t)$$

where $\overrightarrow{E}(t)$ is the electric field ($e = m_e = \hbar = 1$; atomic units).

The total wave function of the molecule can be written as

$$\Psi(t) = \phi_X \psi_X(t) + \phi_A \tilde{\psi}_A(t)$$

where the $\psi_X(t)$ and $\tilde{\psi}_A(t)$ are the nuclear, while the ϕ_X and ϕ_A are the electronic wave functions.

Inserting $\Psi(t)$, we obtain for the nuclear motion

$$\left[\begin{pmatrix} \hat{T} & 0 \\ 0 & \hat{T} \end{pmatrix} + \begin{pmatrix} V_X & \vec{d}(R)\cdot\vec{E}(t) \\ \vec{d}(R)\cdot\vec{E}(t) & V_A \end{pmatrix}\right]\begin{pmatrix} \psi_X(t) \\ \tilde{\psi}_A(t) \end{pmatrix} = i\begin{pmatrix} \dot{\psi}_X(t) \\ \dot{\tilde{\psi}}_A(t) \end{pmatrix}.$$

One can assume (without loss of generality) the following form for the $\tilde{\psi}_A(t)$

$$\tilde{\psi}_A(t) = \psi_A(t)e^{-i\omega_L t}.$$

Substituting it into the TDNSE and performing some algebra yields an identical form for the TDNSE:

$$\left[\begin{pmatrix} \hat{T} & 0 \\ 0 & \hat{T} \end{pmatrix} + \begin{pmatrix} V_X & \vec{d}(R)\cdot\vec{E}(t)e^{-i\omega_L t} \\ \vec{d}(R)\cdot\vec{E}(t)e^{i\omega_L t} & V_A-\omega_L \end{pmatrix}\right]\begin{pmatrix} \psi_X(t) \\ \psi_A(t) \end{pmatrix} = i\begin{pmatrix} \dot{\psi}_X(t) \\ \dot{\psi}_A(t) \end{pmatrix}.$$

Now we explicitly give the form for the light-matter coupling term

$$\overrightarrow{d}(R) \cdot \overrightarrow{E}(t) = d(R) \cdot \epsilon_0 f(t) \cos\omega_L t \cdot \cos\theta = \frac{d(R) \cdot \epsilon_0 f(t) \cos\theta}{2} \left(e^{-i\omega_L t} + e^{+i\omega_L t} \right).$$

With this we arrive to the final form of the TDNSE

$$\left[\begin{pmatrix} \hat{T} & 0 \\ 0 & \hat{T} \end{pmatrix} + \begin{pmatrix} V_X & \frac{d(R)\epsilon_0 f(t) cos\theta}{2} \left(e^{-2i\omega_L t} + 1 \right) \\ \frac{d(R)\epsilon_0 f(t) cos\theta}{2} \left(e^{+2i\omega_L t} + 1 \right) & V_A - \omega_L \end{pmatrix} \right] \begin{pmatrix} \psi_X(t) \\ \psi_A(t) \end{pmatrix} \tag{1}$$

For molecules with two electronic states this equation provides the **exact solution** for the **nuclear dynamics**.

As long as the $e^{+2i\omega_L t}$ and $e^{-2i\omega_L t}$ terms are neglected in the "exact" Hamiltonian we arrive to the so called rotating wave approximation (RWA).

This approximation has been successfully used for a long time to discuss two level systems, mostly for atoms, when moderate laser field intensities are applied.

The RWA Hamiltonian is:

$$\left[\begin{pmatrix} \hat{T} & 0 \\ 0 & \hat{T} \end{pmatrix} + \begin{pmatrix} V_X & \frac{d(R)\epsilon_0 f(t) cos\theta}{2}. \\ \frac{d(R)\epsilon_0 f(t) cos\theta}{2} & V_A - \omega_L \end{pmatrix}\right].$$

Taking the value of the $f(t)$ **envelope** function **equal to one** in the Hamiltonian of the **RWA** we arrive to the **Floquet** approximation. In this sense, these **two methods** are **equivalent** to each other.

G. J. Halász, Á. Vibók, N. Moiseyev and L. S. Cederbaum: *J. Phys. B*. **45**, 135101, (2012).

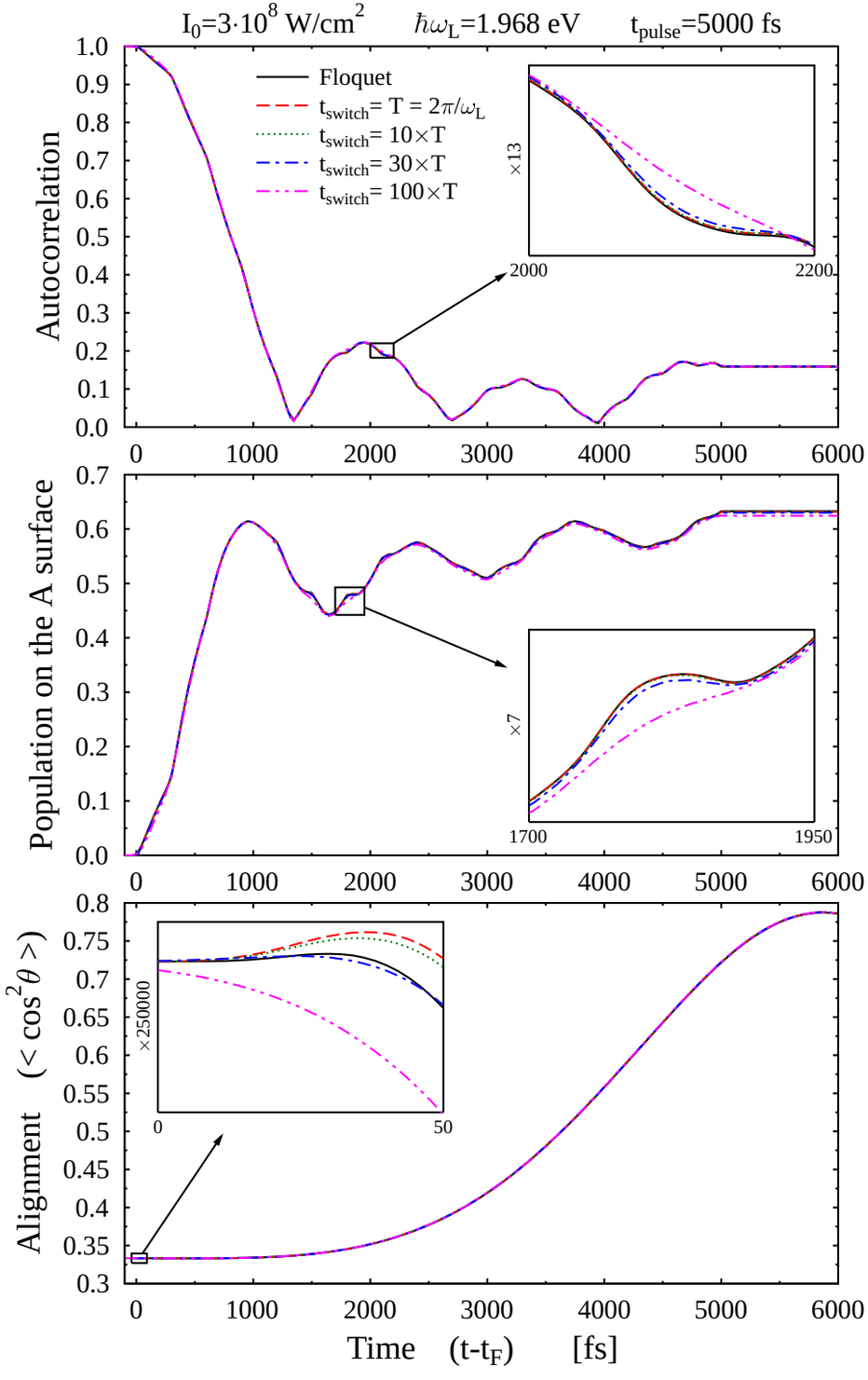
I0=3·10^8 W/cm^2
ħωL=1.968 eV
tpulse=5000 fs
Floquet
tswitch= T = 2π/ωL
tswitch= 10×T
tswitch= 30×T
tswitch= 100×T
Autocorrelation
×13
2000
2200
Population on the A surface
×7
1700
1950
Alignment (< cos^2θ >)
×250000
0
50
Time (t-tF) [fs]

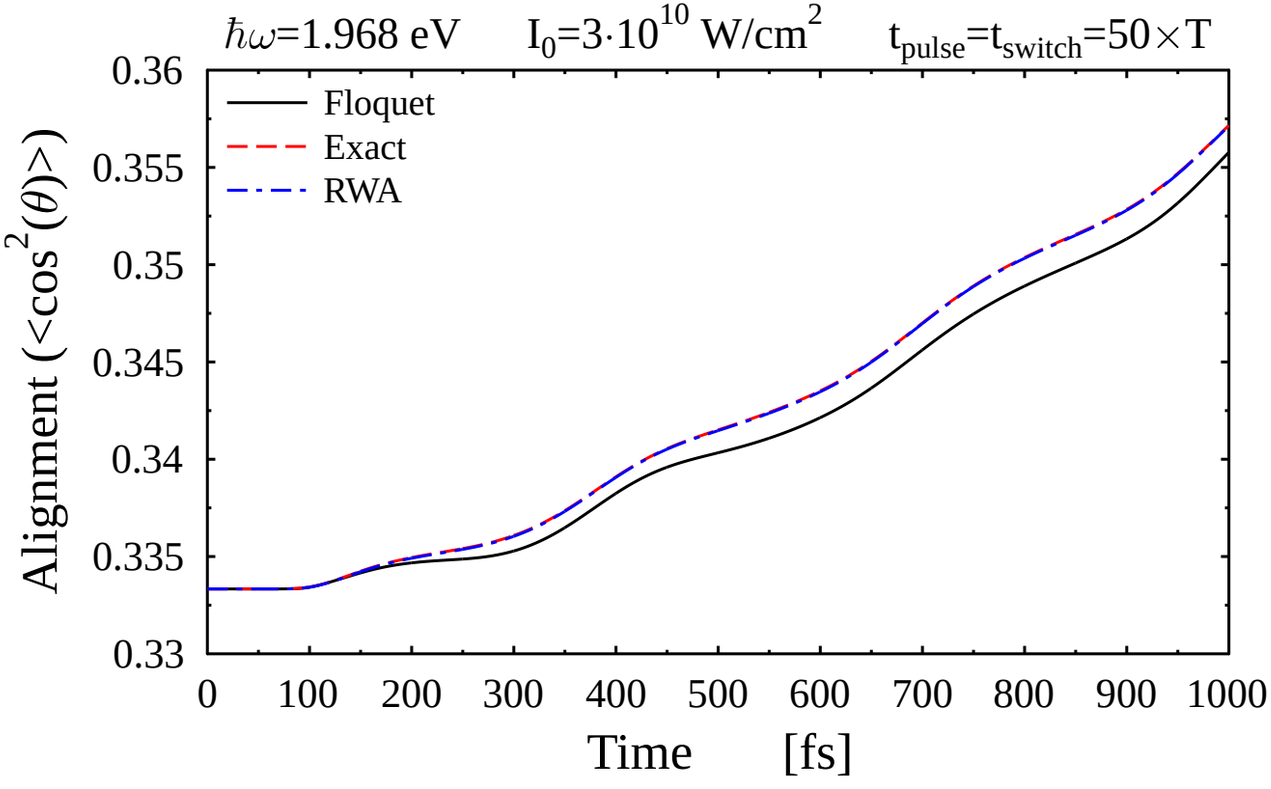
ħω=1.968 eV
I0=3·10^10 W/cm^2
tpulse=tswitch=50×T
Floquet
Exact
RWA
Alignment (<cos^2(θ)>)
0.36
0.355
0.35
0.345
0.34
0.335
0.33
0
100
200
300
400
500
600
700
800
900
1000
Time [fs]

Photodissociation dynamics of the D_2^+ molecule

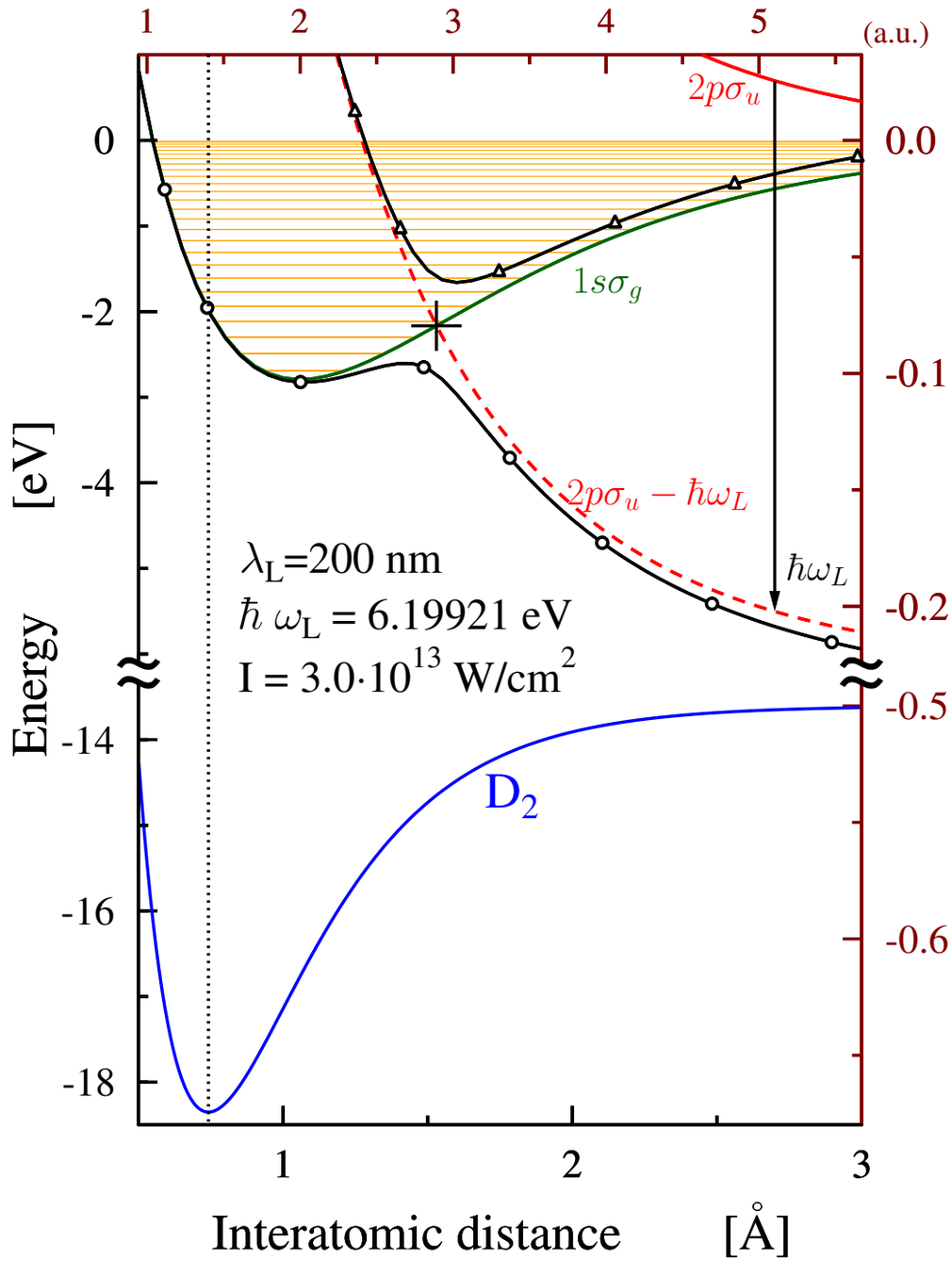
1
2
3
4
5
(a.u.)
$2p\sigma_u$
$1s\sigma_g$
$2p\sigma_u - \hbar\omega_L$
$\hbar\omega_L$
λ_L=200 nm
$\hbar\,\omega_L$ = 6.19921 eV
I = 3.0·10^{13} W/cm^2
D_2
0
-2
-4
-14
-16
-18
[eV]
Energy
0.0
-0.1
-0.2
-0.5
-0.6
1
2
3
Interatomic distance
[Å]

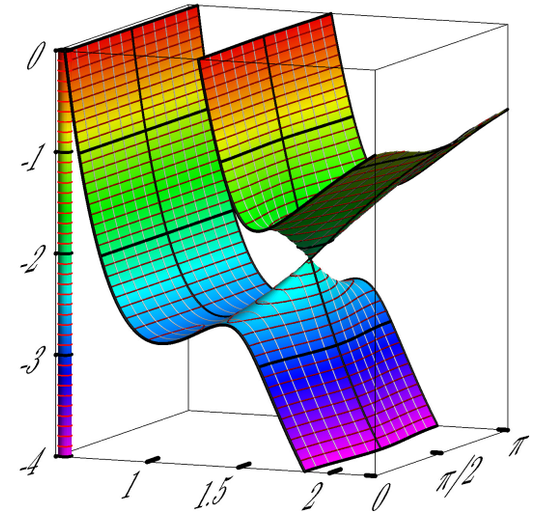
0
-1
-2
-3
-4
1
1.5
2
0
π/2
π

Kinetic Energy Release (KER)(FC)

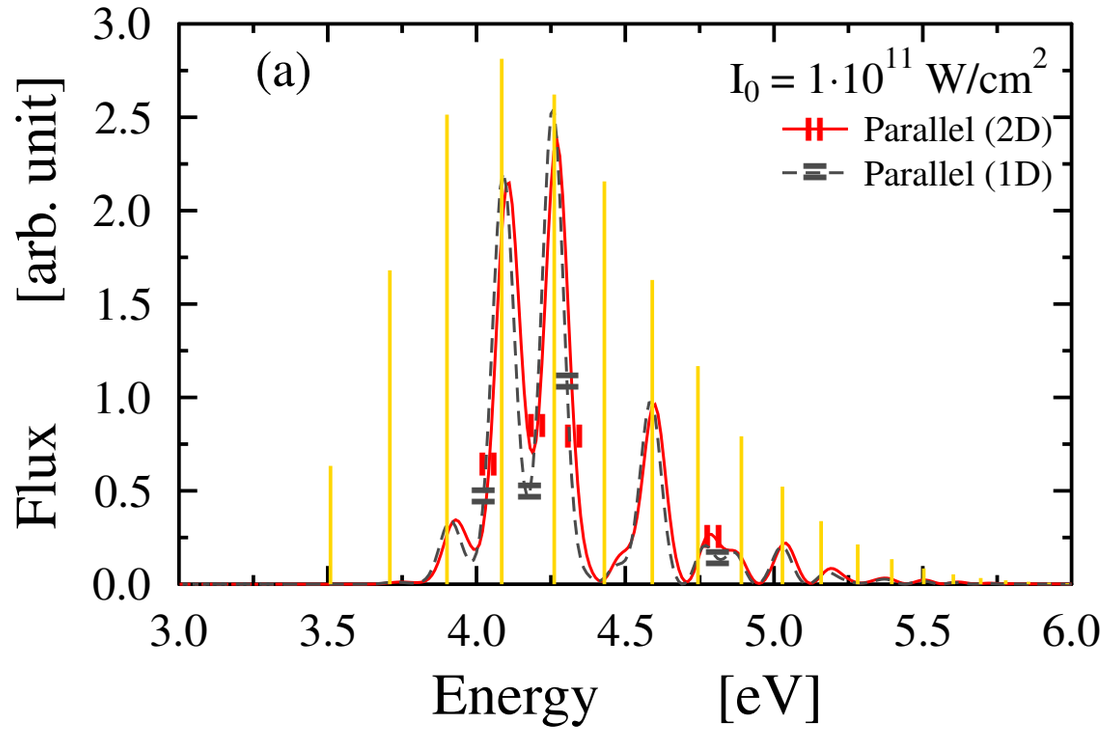

1D and 2D calculations are practically the same. There is no rotation for this initial orientation.

G. J. Halász, Á. Vibók, H.-D. Meyer and L.S. Cederbaum, *J. Phys. Chem. A.* ***117***, *8525, (2013).*

Kinetic Energy Release (KER)(FC)

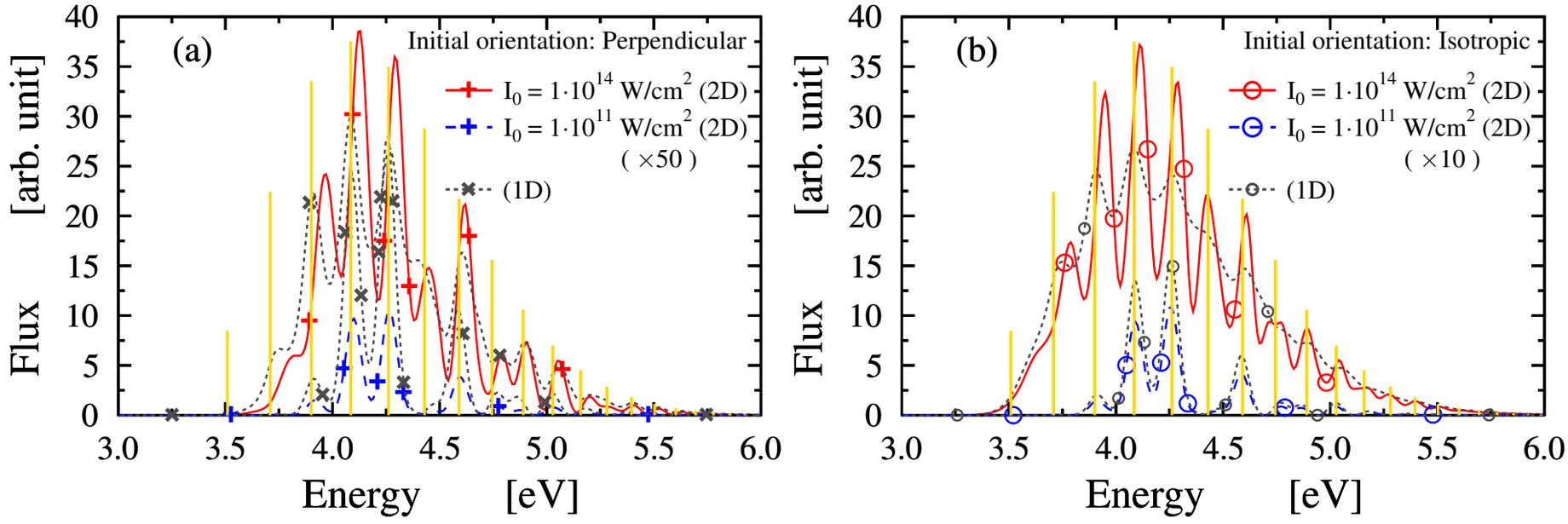

The 1D and 2D results are very different! The rotation has a very significant role for these geometrical arrangements. The dissociation probability is strongly dependent on the initial alignment.

G. J. Halász, Á. Vibók, H.-D. Meyer and L.S. Cederbaum, *J. Phys. Chem. A.* ***117***, *8525, (2013).*

Kinetic Energy Release (KER)(FC)

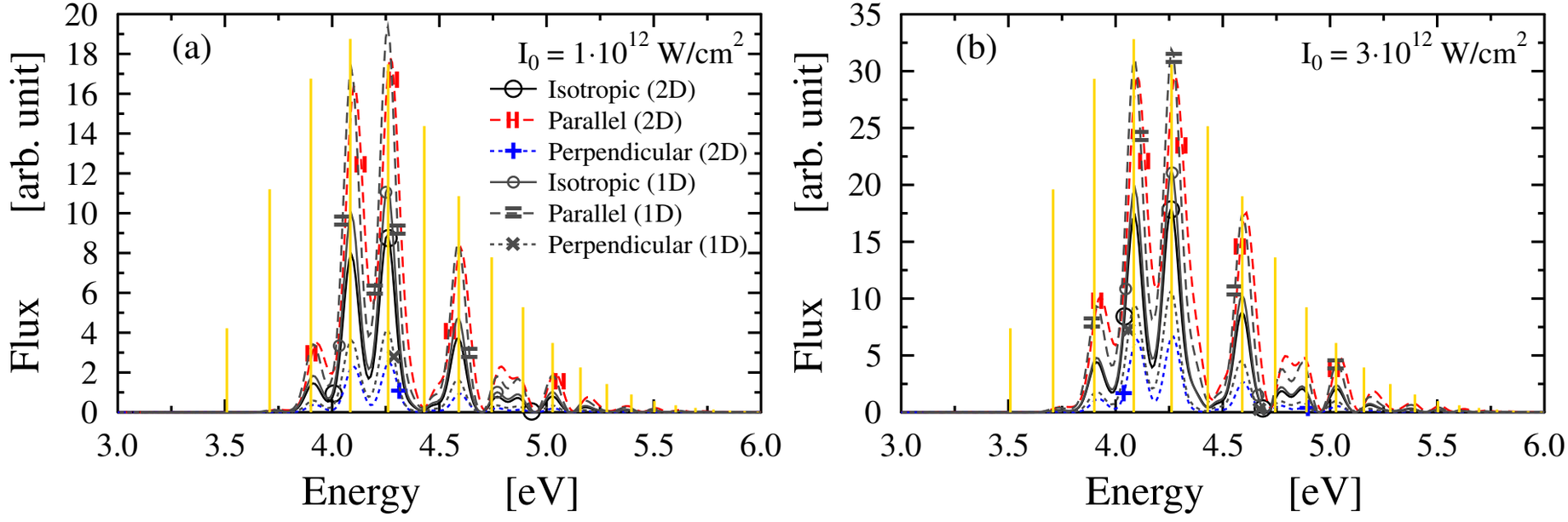

Below the intensity of 1×10^{13}W/cm^2 the dissociation probability of the $\nu = 5$ is practically zero. Fragment energies from this eigenstate are missing in the spectra.

G. J. Halász, Á. Vibók, H.-D. Meyer and L.S. Cederbaum, *J. Phys. Chem. A.* ***117***, *8525, (2013).*

Angular Distribution (FC)

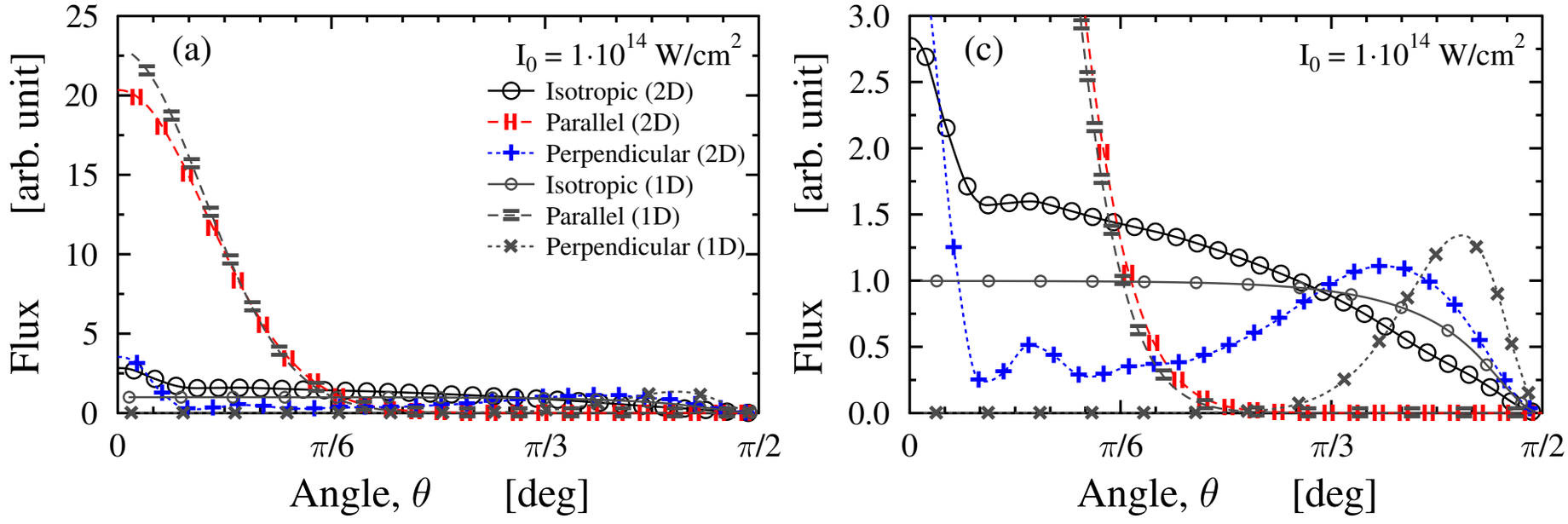

For larger intensities characteristic humped structure in the full 2D curves (isotropic and perpendicular). There are no additional patterns in 1D.

G. J. Halász, Á. Vibók, H.-D. Meyer and L.S. Cederbaum, *J. Phys. Chem. A.* ***117***, *8525, (2013).*

Angular Distribution (FC)

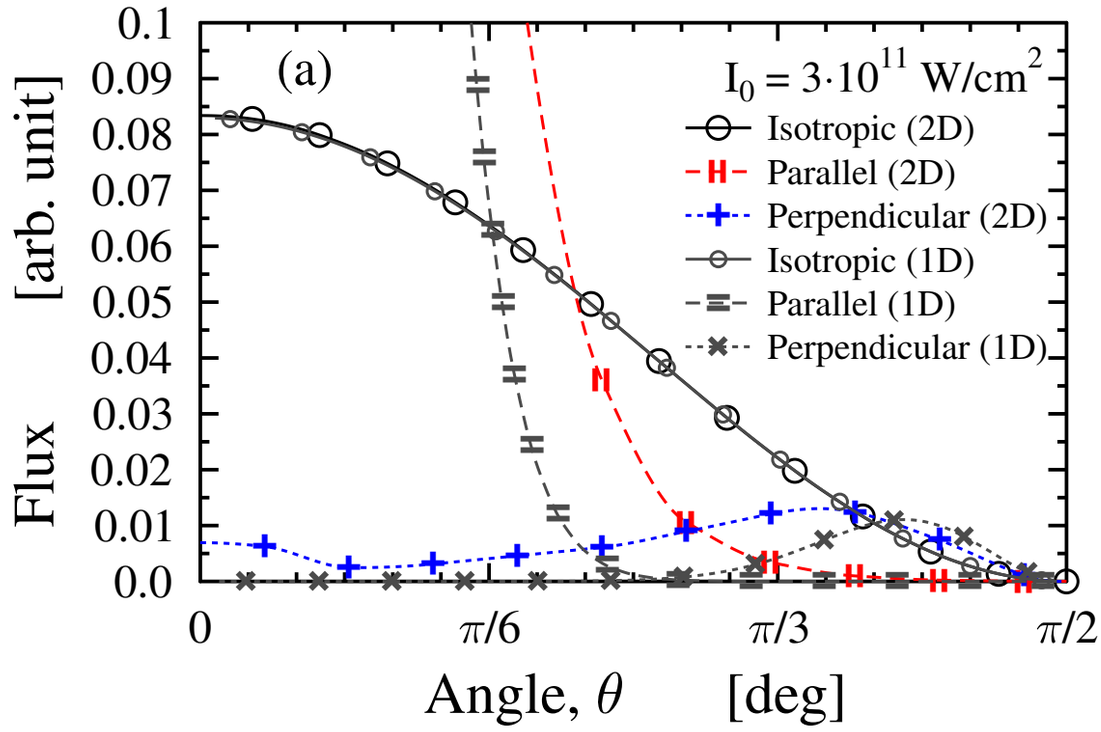

Curves are smooth both for the 1D and 2D calculations.

G. J. Halász, Á. Vibók, H.-D. Meyer and L.S. Cederbaum, *J. Phys. Chem. A.* ***117***, *8525, (2013).*

Angular Distribution (ν)

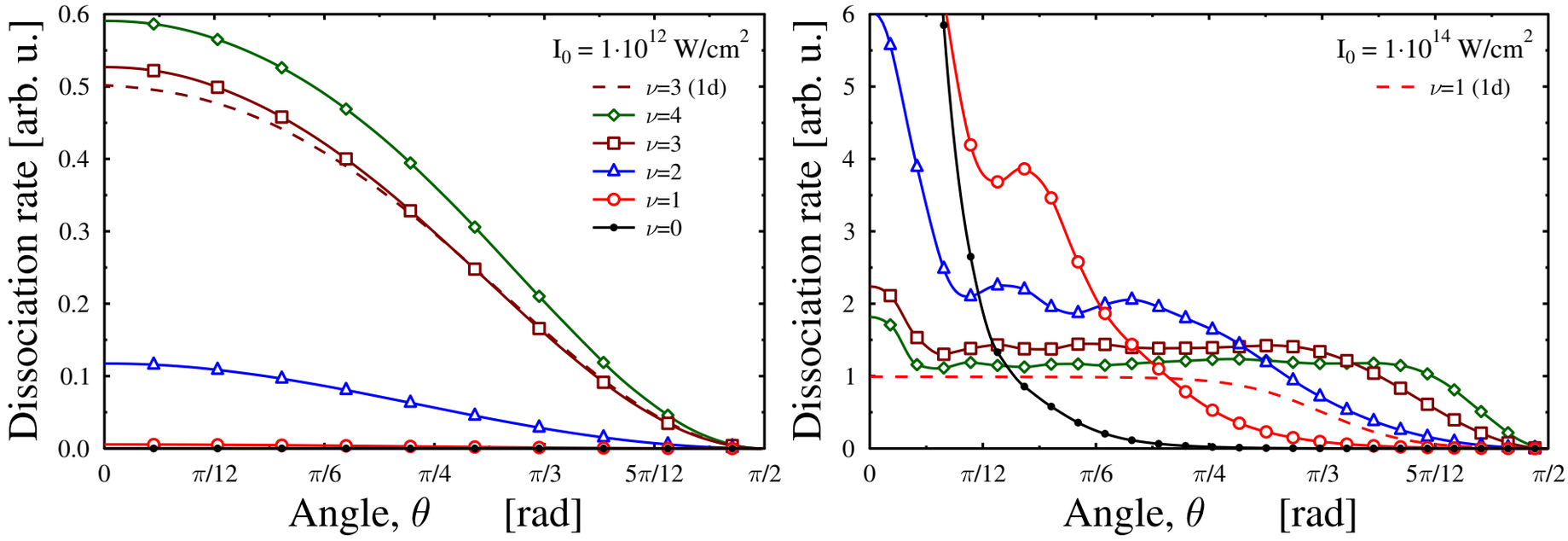

Again, curves are smooth for low intensities and bumpy structured for high intensities.

G. J. Halász, Á. Vibók, N. Moiseyev and L.S. Cederbaum, *PRA* ***88***, *043413, (2013).*

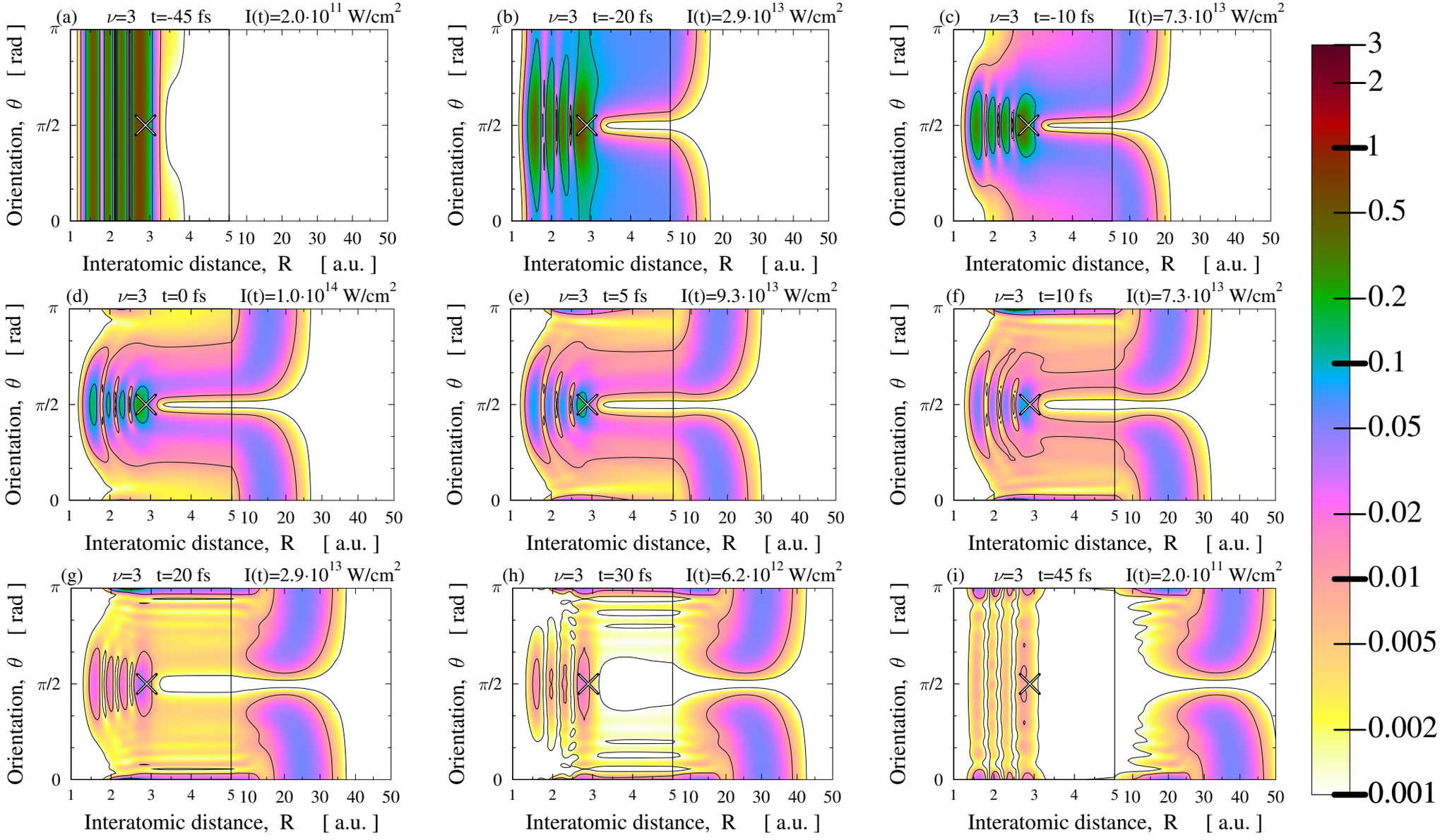

Snapshots from the real-time evolution of the interference appearing in the angular distribution of the dissociated particles. I=$1 \times 10^{14} W/cm^2$ intensity and $\nu = 3$ vibrational state are applied. The cross denotes the position of the LICI.

G. J. Halász, Á. Vibók, N. Moiseyev and L.S. Cederbaum, *PRA* ***88***, *043413, (2013).*

First experimental observation

Experimental Observation of Light Induced Conical Intersections in a Diatomic Molecule

Adi Natan, Matthew R Ware, Philip H Bucksbaum

Stanford PULSE Institute, SLAC National Accelerator Laboratory, 2575 Sand Hill Rd. Menlo Park, CA, 94025, USA, and Department of Physics, Stanford University, Stanford, CA, 94305, USA

natan@stanford.edu

Abstract: We observe quantum interferences in the angular distributions of H_2^+ photodissociation arising from the geometric singularity induced by strong laser fields. This is the first experimental observation of light induced conical intersections in diatomic molecules.

OCIS codes: 020.2649 , 320.2250.

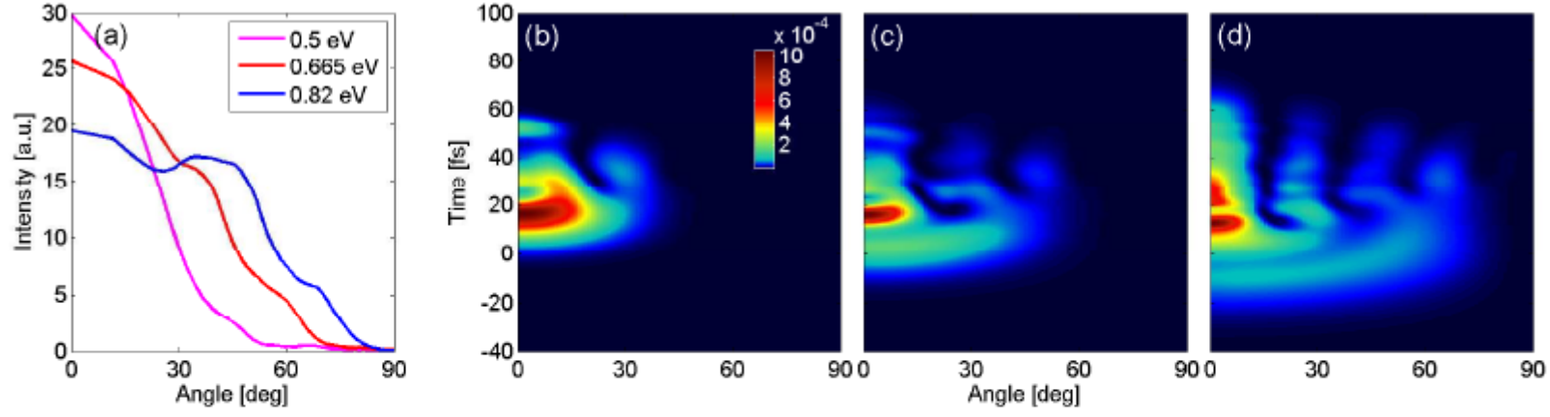

Fig. 1. (a) Measured dissociation yield vs Angle of H_2^+ for kinetic energy release values that correspond to levels $v = 7, 8, 9$ reveal modulations at different angles. (b-d) Calculated disassociation probability as function of time and angle for molecules that were initialized in the (b) $v = 7$, (c) $v = 8$ and (d) $v = 9$ vibrational eigen-states, in the ground rotational state $j = 0$. Peak intensity of pulse happens at $t = 0$fs.

Kinetic Energy Release (KER)(ν)

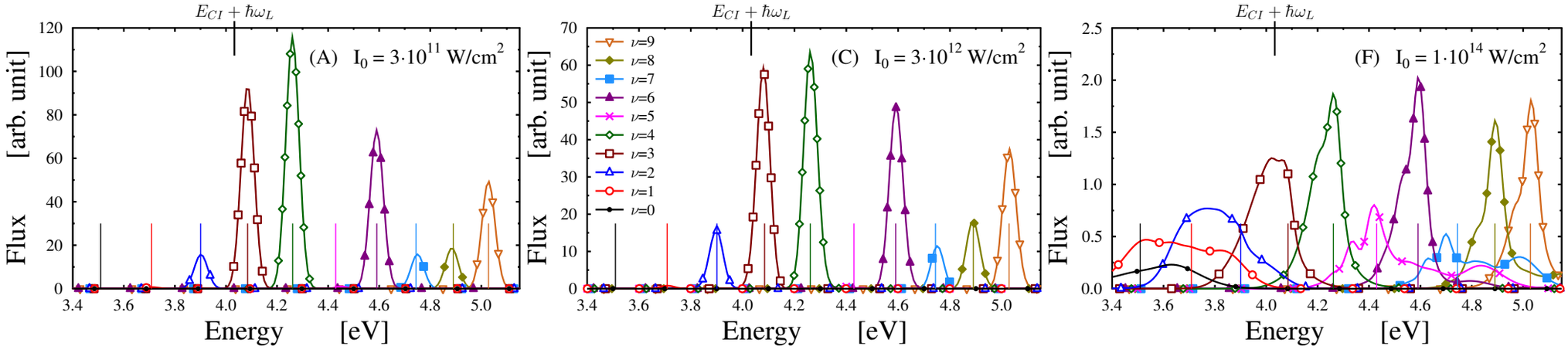

For lower intensities the dissociation probability from $\nu = 5$ is very small (practically zero). From $\sim 10^{13}$W/cm^2 the flux starts to grow, but its value still remains moderate even at the largest 10^{14}W/cm^2 intensity.

G. J. Halász, A. Csehi, Á. Vibók and L.S. Cederbaum, *J. Phys. Chem. A. dx.doi.org/10.1021/jp504889e (2014).*

- Light-induced conical intesection (LICI)

- Adiabatic-diabatic picture

- Bond softening and bond hardening (vibrational trapping) effects

- These are not enough to understand the dissociation mechanism....

- The shape of the adiabatic PESs are depend on the intensity and energy of the applied laser field. Therefore the quasi-bound states of the adiabatic PES are also depend on them

- Changes in these parameters will shift the energy of the quasi-bound states...

- There is no flux in the spectra from a certain vibrational state, if the energy of the vibrational wave packet is very close or is the same, as the energy one of the quasi bound eigenstates in the upper adiabatic potential

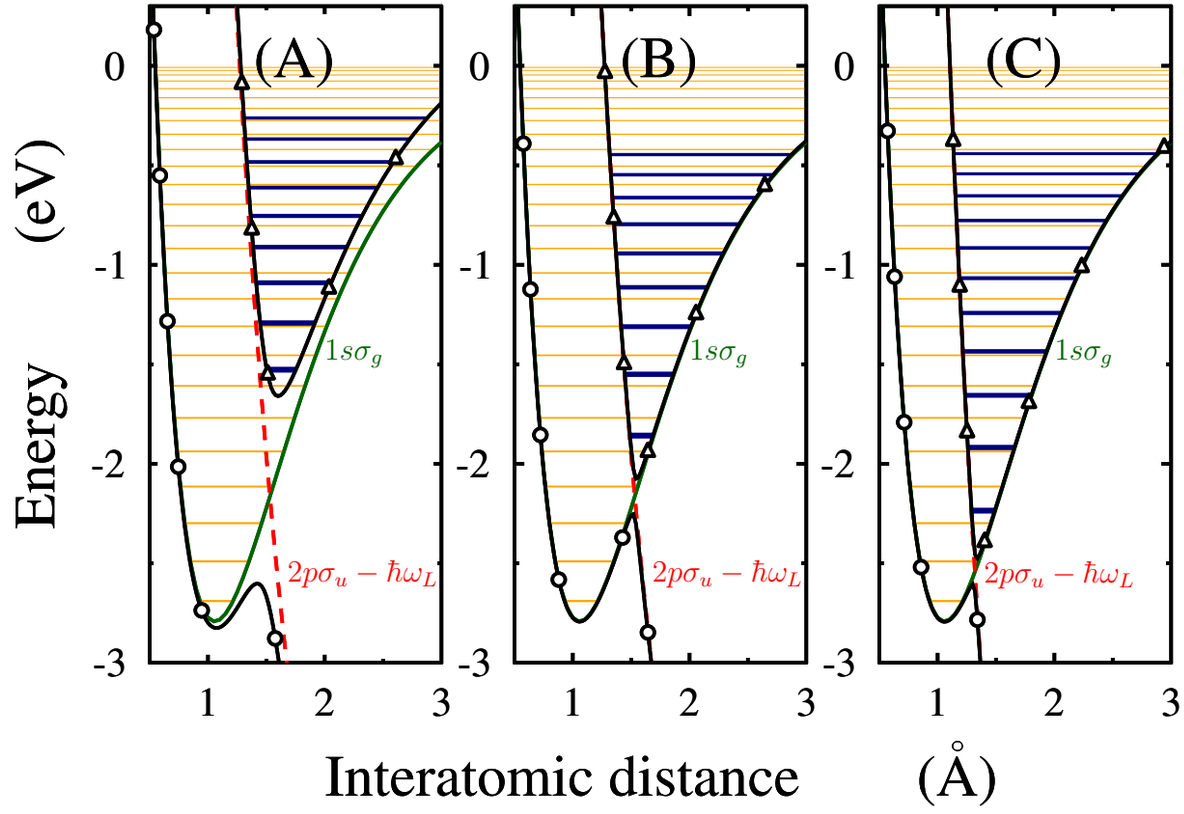

G. J. Halász, A. Csehi, Á. Vibók and L.S. Cederbaum, *J. Phys. Chem. A. dx.doi.org/10.1021/jp504889e (2014).*

Aubanel, E. E.; Gauthier, J. M. and Bandrauk, A. D.. Phys. Rev. A (1993), ***48****, 2145-2152.*

Dissociation Probability (1D)

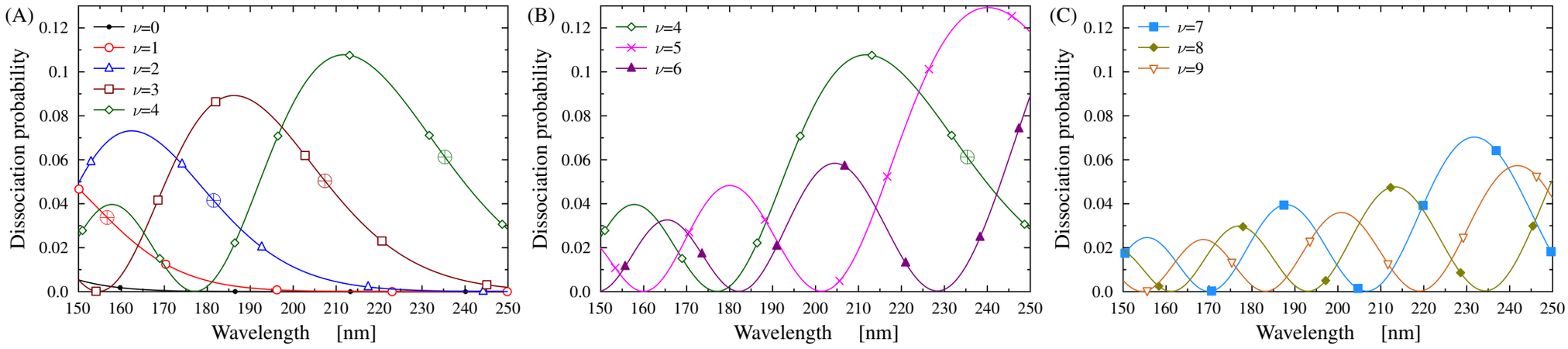

Several pairs of wavelengths and vibrational quantum numbers exist in the studied parameter interval for that the values of the flux are close to zero.

G. J. Halász, A. Csehi, Á. Vibók and L.S. Cederbaum, *J. Phys. Chem. A. dx.doi.org/10.1021/jp504889e (2014).*

Summary

1. Diatomic molecules exhibit CIs which are induced by laser waves.

2. In this case the rotational and vibrational degrees of freedom provide the 2 dimensional branching space.

3. These CIs have strong impact on the molecular dynamics, alignment, dissociation probability...and could also be strong impact on other physical quantities.

4. The energetic position of this CI can be controlled by the laser frequency and the strength of its NACs by the laser intensity.

5. In polyatomic systems CIs are given by nature and induced by laser light can interplay and will lead to a wealth of new phenomena.

Future

1. LICI in polyatomic molecule. Ozone...

2. LICI created by chirped laser pulse...

3. Towards the full dynamical description of D_2^+ in intense laser field. Dissociation and ionization...

Collaborators

Theory

- **Gábor Halász** (University of Debrecen);
- Fabien Gatti, Benjamin Lasorne, Aurelie Perveaux (University of Montpelier, France);
- David Lauvergnat (University Paris-Sud);
- Michael A Robb (Imperial College London);
- **Lenz Cederbaum**, Hans-Dieter Meyer (Univ. Heidelberg);
- Nimrod Moiseyev (Technion, Israel);

Experiment

- Reinhard Kienberger, Michael Jobst, Ferenc Krausz (Max Planck Institute, Garsching, Germany);

Grants and financial support

- MTA-CNRS;

- Munich-Centre for Advanced Photonics;

- Cluster of Excellence of the German Research Foundation (DFG);

- This research was supported by the European Union and the State of Hungary, co-financed by the European Social Fund in the framework of TÁMOP-4.2.4.A/ 2-11/1-2012-0001 ‘National Excellence Program’;

European Cooperation in Science and Technology

Thank you for your attention!

A projekt az Európai Unió támogatásával, az Európai Regionális Fejlesztési Alap társfinanszírozásával valósul meg.